Mass systematics for $A=29-44$ nuclei: The deformed $A\sim32$ region

E. K. Warburton
Brookhaven National Laboratory, Upton, New York 11973
and Universität Heidelberg and the Max-Planck-Institut für Kernphysik, Heidelberg, West Germany

J. A. Becker
Lawrence Livermore National Laboratory, Livermore, California 94550

B. A. Brown
Cyclotron Laboratory and Department of Physics and Astronomy, Michigan State University, East Lansing, Michigan 48824
(Received 11 October 1989)

Further evidence for the presence of an anomaly in binding energies for the "island of inversion" centered at $Z=11$, $N=21$ is obtained by comparison of shell-model calculations to experiment. The calculations were done with a shell-model interaction that is applicable to nuclei with active valence nucleons in both the $(1s,0d)$ and $(0f,1p)$ major shells. This interaction is described in detail as are its predictions for binding energies and energy spectra of $Z=8-20$, $N=18-25$ nuclei. These calculations provide the background for the exploration of the "island of inversion." The extent of the "island" and the magnitude of the anomaly is explored by calculating the binding energies of $2\hbar\omega$ excitations of neutrons from the $(1s,0d)$ shell to the $(0f,1p)$ shell relative to the $0\hbar\omega$ ground state. The reason why mixed $(0+2)\hbar\omega$ calculations are not considered reliable is addressed. Truncation schemes and a weak-coupling approximation are used to extend the range of the calculations. It is found that for $Z=10-12$, $N=20-22$ (and possibly $N>22$) nuclei the lowest $2\hbar\omega$ state is more bound than the $0\hbar\omega$ ground state. The role of odd n $n\hbar\omega$ excitations is considered and it is found that the $1\hbar\omega$ ground state always lies below that of $3\hbar\omega$, and for $N=19$, 21, and 23, the lowest $1\hbar\omega$ state is in close competition with $2\hbar\omega$ for the lowest binding energy. Collectivity is considered via $E2$ observables and energy spectra for the $2\hbar\omega$ ground-state bands. The reason for the existence of the "island" is discussed.

I. INTRODUCTION

The observation of irregularities in the binding energies of neutron-rich $A\simeq32$ nuclei and the suggestion that this might be due to deformation was first made by Thibault *et al.*[1] These authors measured the binding energies of $^{27-32}$Na isotopes and noted that ^{31}Na and ^{32}Na were considerably more bound than predicted theoretically. Campi *et al.*[2] performed constrained Hartree-Fock calculations on these Na isotopes and obtained results supporting this hypothesis. In particular they found large prolate deformations in ^{31,32}Na when promotion of neutrons from the $d_{3/2}$ orbit to the $f_{7/2}$ orbit was allowed. Later, mass measurements[3] were extended to include the Mg isotopes up to ^{32}Mg, and both ^{31}Mg and ^{32}Mg were also found to be a great deal more bound than expected. In addition, the first-excited state of ^{32}Mg—assumed to be 2^+—was found to lie at the remarkably low energy of 885 keV, clearly indicating nuclear deformation.[4]

Investigation of the anomalies in the $A\simeq32$ region via the shell model got underway when Chung and Wildenthal[5] showed that the binding energies of the $N=20$ Na and Mg isotones could not be understood on the basis of the best available shell-model interaction with the active orbits constrained to the $(1s,0d)$ major shell alone. They spoke of an "island of inversion" which we illustrate schematically in Fig. 1. The first shell-model calculations of these nuclei which allowed excitations of $(1s,0d)$ neutrons into the $(0f,1p)$ major shell were carried out by Watt *et al.*[6] They were successful in reproducing the general trend of binding energies for the Na and Mg isotopes in the $A=29-34$ region. They undertook a mixed $(0+2)\hbar\omega$ calculation with the $2\hbar\omega$ model space truncated to $\pi d_{5/2}^{Z-8}\nu d_{3/2}^{N-18}f_{7/2}^2$, but with estimates of the effect of contributions from outside this space. Poves and Retamosa[7] carried out similar calculations in the expanded $2\hbar\omega$ space $\pi d_{5/2}^{Z-8}\nu d_{3/2}^{N-18}(f_{7/2},p_{3/2})^2$, i.e., the $\nu p_{3/2}$ orbit was added. They also examined the $E2$ properties of the nuclei considered.

By now there is a general consensus that deformations caused by np-nh neutron excitations increase the binding of $Z\simeq10-12$, $N\simeq20$ nuclei; and it is of interest to consider the origin of these excitations. There appear to be two contributing factors. Storm, Watt, and Whitehead[8] emphasized the effect of the large neutron excess on the *effective* single-particle energies. With their interaction[6] they found that for $Z=8$ or 9, the effective $\nu f_{7/2}$ energy actually drops below the $\nu d_{3/2}$ energy at $N=20$. As we will show (see Sec. V A), we do not find so drastic an effect but certainly the diminishing of the $\nu f_{7/2}-\nu d_{3/2}$ energy gap with neutron excess for $Z=8-12$ nuclei is a

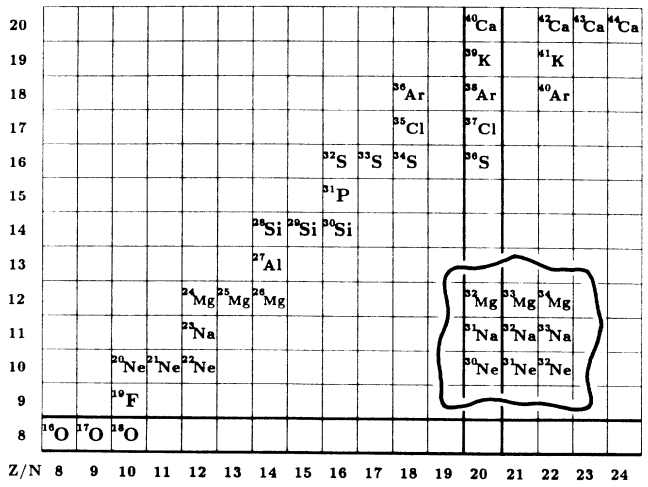

FIG. 1. Partial periodic table highlighting the "island of inversion" centered at ^{32}Na. The extent of the "island" is an important aspect of the study. The magic numbers $Z=8$ and $N=20$ are emphasized with double lines. Apart from the "island," only stable nuclei are shown.

contributing factor. However, the major factor would appear to be the very strong effect of the $T=0$ proton-neutron (p-n) interaction for just the region in question. The crucial role of this interaction in forming deformations throughout the periodic table was emphasized by De-Shalit and Goldhaber[9] and later by Federman and Pittel.[10] The interaction is proportional to the overlap between neutron and proton orbitals and thus is strong when $n_p \simeq n_n$ and $l_p \simeq l_n$ as is certainly the case for the interaction of the $\pi 0d_{5/2}$ orbit with the $\nu 0d_{3/2}$ orbit and, to a large extent, with the $\nu 0f_{7/2}$ orbit also. The interaction is strongest for spin-orbit partners. Poves and Retamosa[7] discussed a "correlation energy" for $(1s,0d)^{-2}(0f,1p)^2$ configurations. They did not give a quantitative definition of this "correlation energy" but it presumably contains the effect of the p-n interaction. For $N=20$, this energy was found to be close to zero for $Z=8$ and 14, and to vary parabolically in between with a minimum of ~ 4.5 MeV at $Z=11$. This is just as expected for the interaction of $\pi d_{5/2}^{Z-8}$ with $\nu(1s,0d)^{-2}(0f,1p)^2$; i.e., the energy is directly dependent on the number of active $d_{5/2}$ protons or holes (as is appropriate).

In this paper we report on a shell-model investigation of the $A \simeq 32$ region utilizing an interaction designed to operate in the full $(1s,0d)(0f,1p)$ model space. There are several reasons why we feel another approach is desirable. Firstly, the two previous shell-model investigations[6,7] used interactions specifically constructed for the problem at hand and it is difficult to estimate the uncertainties in their binding energies since systematic calculations over a range of nuclei were not performed. Secondly, in both investigations, calculations were done in a mixed $(0+2)\hbar\omega$ space. There is a serious problem with such calculations which we shall term the "$n\hbar\omega$ truncation catastrophe" and which we now describe.

Since the expansion of shell-model wave functions in an $n\hbar\omega$, $n=0,2,4,\ldots$ model space is slowly converging and the dimensions increase rapidly with n, one conventionally resorts to an effective interaction—formulated in the $0\hbar\omega$ space—in which an attempt is made to account for the gross properties of the rest of the series in an approximate way. The slow convergence also has the consequence that the "$n\hbar\omega$ truncation catastrophe" occurs if the series is terminated at $2\hbar\omega$. The difficulty is that there is a very strong interaction between the low-lying $0\hbar\omega$ states and the $2\hbar\omega$ states which have similar symmetries, even though the latter lie at high energy (~ 20 MeV in ^{16}O), with the consequence that the $0\hbar\omega$ states are pushed considerably lower in energy by this interaction.[11-13] If dimensional considerations were not a problem, one could restore the "correct" relative binding energies—at least partially—by including $4\hbar\omega$ configurations in the model space. But, the fact remains that in mixed $(0+2)\hbar\omega$ calculations not only are the binding energies grossly in error but also the mixing between the two $n\hbar\omega$ spaces is wrong because it depends on the perturbed energies. This discussion of the "catastrophe" is most relevant to calculations in which all orbits of the two major shells are fully active. If not, then the $2\hbar\omega$ states of the same symmetry will not be fully present. Thus, it is possible to avoid the most obvious symptom of this phenomenon—the large depression of the ground-state binding energy—by severe truncation of the model space. This, of course, causes even greater problems. For instance, the $2\hbar\omega$ components mixed into the low-lying $0\hbar\omega$ states will not include the large contribution from the $2\hbar\omega$ components of similar symmetry (which would be present in a "full" calculation), or, if the truncation is intermediate, then it is difficult to ascertain just how much of the binding energy depression still remains and thus it is difficult to obtain reliable binding energies.

For the reasons just described we shall diagonalize the $0\hbar\omega$ and $2\hbar\omega$ space separately. In their seminal study of $(0+2)\hbar\omega$ mixing in ^{16}O, Ellis and Zamick[11] suggested that this procedure probably gives the most reliable estimate of the binding energies of the predominantly $0\hbar\omega$ and predominantly $2\hbar\omega$ states and our experience in calculations near ^{16}O and ^{40}Ca supports this suggestion. Since our study is based on calculations in a full $(1s,0d)(0f,1p)$ model space (or as close to it as possible) the number of nuclei in the $A \simeq 32$ region for which we can consider coexisting $0\hbar\omega$ and $2\hbar\omega$ states is limited, but it is very worthwhile to consider these in some detail. In order to explore the $2\hbar\omega$ binding energy systematics for a larger region of Z and N, we must resort to truncation schemes. We also find that a simple weak-coupling model for the excitation energies is a very good approximation to the full calculations. With this weak-coupling model we are able to delineate the binding energy systematics for $Z=8-20$, $N=20-22$ nuclei and some $N=23$ nuclei as well.

The interaction used is described in Sec. II. Binding energy calculations of neutron-rich states in the $A=31-44$ region are presented in Sec. III where we also compare these results to experiment. Coexisting $0\hbar\omega$ and $2\hbar\omega$ and also $1\hbar\omega$ and $3\hbar\omega$ states of $A \simeq 32$ nuclei are considered in Sec. IV and the results discussed in Sec. V. Our findings are summarized in Sec. VI.

II. THE WBMB INTERACTION

A. Construction of the interaction

The interaction—designated WBMB—was developed by Warburton, Becker, Millener, and Brown[14] for calculations in a $(1s,0d)^{A-16-n}(0f,1p)^n$ model space with a single value of n. We shall label this model space for specific A as nfp. It is not recommended for calculations with mixed values of n. The reasons are discussed in Sec. I. It is derived from an effective one-body plus two-body Hamiltonian and is composed of three parts. The starting point is the "universal" $(1s,0d)$ interaction—denoted USD—of Wildenthal.[15] Interactions between $(0f,1p)$ nucleons are accounted for by an interaction developed by McGrory[16] and the cross-shell interaction connecting the $(1s,0d)$ and $(0f,1p)$ shells was generated from the nucleon-nucleon potential of the Millener-Kurath interaction.[17] We first describe these three interactions in more detail. We briefly touch on modifications made to the Millener-Kurath interaction in order to obtain better agreement with the $T=0$ and 1 particle-hole spectra of ^{40}Ca. Finally we describe how the three interactions are connected.

Wildenthal's USD interaction. The parameters of this interaction consist of 63 two-body matrix elements (TBME) and three single-particle energies (SPE) relative to the ^{16}O core. These were determined from a least-squares fit to ~440 binding energies in $A=18$–39 nuclei. In this fit, the SPE were constrained to be independent of A and the TBME were given an A-dependence of $A^{-0.3}$. The final results had an rms deviation for the ~440 binding energies of 185 keV.[18]

McGrory's (0f,1p) interaction. Assuming a ^{40}Ca core, there are 195 TBME and four SPE necessary to describe the $(0f,1p)$ interaction. The starting point of McGrory's interaction is the $(0f,1p)$ effective interaction of Kuo and Brown.[19] McGrory performed a least-squares fit to 29 binding energies in the $A=42$–44 region with only the eight $\langle f_{7/2}f_{7/2}|V|f_{7/2}f_{7/2}\rangle_{JT}$ TBME variable. All TBME and SPE were assumed to be mass independent and the relative SPE were set at 0, 2.1, 3.9, and 6.5 MeV for the $0f_{7/2}$, $1p_{3/2}$, $1p_{1/2}$, and $0f_{5/2}$ orbits, respectively. The justification for this procedure and results for $A=42$–44 nuclei are described in detail by McGrory.[16]

The cross-shell interaction. The Millener-Kurath particle-hole interaction was developed to describe non-normal parity states in the $A=16$ region. The necessary TBME were generated from a potential

$$
\begin{aligned}
&V(r)=V_c(r)+V_{LS}(r)+V_T(r)\ ,\\
&V_c(r)=V_c[\Delta_c^{11}P^{11}+\Delta_c^{31}P^{31}+\Delta_c^{13}P^{13}+\Delta_c^{33}P^{33}]f_c(r)\ ,\\
&V_{LS}(r)=V_{LS}[\Delta_{LS}^{13}P^{13}+\Delta_{LS}^{33}P^{33}]\mathbf{L}\cdot\mathbf{S}f_{LS}(r)\ ,\\
&V_T(r)=V_T[\Delta_T^{13}P^{13}+\Delta_T^{33}P^{33}]S_{12}f_T(r)\ ,
\end{aligned}
\tag{1}
$$

where V_c, V_{LS}, and V_T are central, spin-orbit, and tensor terms. The $P^{2T+1,2S+1}$ are projection operators, the $\Delta^{2T+1,2S+1}$ describe the exchange mixture, $V<0$ corresponds to an attractive force, the tensor operator S_{12} is as defined by Cohen and Kurath,[20] and by convention $\Delta_c^{13}\equiv 1$. Millener and Kurath used a Yukawa form—$\exp(-x)/x$ (with $x=r/\mu$)—for all the $f(r)$ with $b/\mu=1.18$ for $f_c(r)$ and $f_T(r)$ and 2.36 for $f_{LS}(r)$, where b and μ are the harmonic oscillator and Yukawa range parameters, respectively. A fairly good fit to the $T=0$ and 1 "1p-1h" states of ^{16}O was obtained with the parameters listed in Ref. 17. The choice of the form of the interaction and the values of the parameters were strongly guided by a desire to stay close to the realistic G-matrix interaction of Kuo.[21]

We have used exactly this potential to generate the 510 TBME needed to describe the interaction connecting the $(1s,0d)$ and $(0f,1p)$ shells. The matrix elements were calculated with an oscillator length $b=(41.467/\hbar\omega)^{1/2}$ fm with $\hbar\omega=45A^{-1/3}-25A^{-2/3}$ and with $A=40$ ($\hbar\omega=11.021$ MeV, $b=1.9404$ fm).

A major consideration in the choice of the parameters of the Millener-Kurath potential was its predictions for the "1p-1h" spectrum of ^{16}O. In a similar manner, we are interested in its predictions for the $T=0$ and $T=1$ "1p-1h" states of ^{40}Ca. They are found to be just about as good for ^{40}Ca as for ^{16}O.[22] However, as described in the development of our first version of this interaction,[13] selected crucial TBME were varied to give better agreement with the energy spectra and spectroscopic factors of the "1p-1h" states of ^{40}Ca. Those varied in the present instance were the $\langle d_{3/2}f_{7/2}|V|d_{3/2}f_{7/2}\rangle_{JT}$ and $\langle d_{3/2}p_{3/2}|V|d_{3/2}p_{3/2}\rangle_{JT}$ TBME of which there are eight each. The resulting 16 TBME are compared to the original Millener-Kurath values in Table I. It can be seen that the WBMB TBME in Table I differ very little from the Millener-Kurath values. Since the WBMB values give what we term the "ideal" ^{40}Ca "1p-1h" energy spectrum,[14] this is a satisfactory verification that the Millener-Kurath potential is a quite realistic one.

The connection between the three interactions is some-

TABLE I. Comparison of two-body matrix elements of the WBMB interaction with those derived from the Millener-Kurath potential. Only the sixteen matrix elements that were changed are listed. All energies are in MeV.

J,T	WBMB	Millener-Kurath
	$d_{3/2}f_{7/2}$	
2,0	−3.793	−3.512
3,0	−2.401	−1.967
4,0	−1.490	−0.925
5,0	−2.384	−2.315
2,1	+0.017	+0.366
3,1	+0.217	−0.047
4,1	+0.441	+0.089
5,1	−0.458	−1.086
	$d_{3/2}p_{3/2}$	
0,0	−2.771	−2.952
1,0	−2.697	−2.142
2,0	−1.134	−1.180
3,0	−1.287	−1.254
0,1	+0.582	+0.320
1,1	+0.964	+0.620
2,1	+0.072	+0.080
3,1	−0.365	−0.251

what complicated by the fact that the TBME of the USD interaction have an $A^{-0.3}$ dependence while the McGrory interaction is A independent. For $A \leq 40$ nuclei we adopt the $A^{-0.3}$ dependence for all three interactions, while for $A > 40$ nuclei the TBME of the Millener-Kurath and McGrory interactions are fixed at their $A = 40$ values. One further refinement was made because it was found to give better agreement with experimental binding energies. Namely, in calculations within a $(1s,0d)^{A-16-n}(0f,1p)^n$ model space, the TBME of the USD are given an A dependence appropriate to $A-n$ rather than A.

All that remains to be determined are the single-particle energies (SPE). These are assumed to be independent of A. We use the three USD values for the $0d_{5/2}$, $0d_{3/2}$, and $1s_{1/2}$ orbits and the relative values of McGrory for the four $(0f,1p)$ orbits. This leaves the $(1s,0d)$ to $(0f,1p)$ energy gap to be determined. We started by demanding agreement with the difference between the experimental binding energies of ^{41}Ca and ^{40}Ca, 8363 keV. Later, this energy gap was fixed so as to best describe binding energies of selected levels in the $A = 35-43$ region. As it turned out, that was a quite small change, yielding 8365 keV for the energy difference between ^{41}Ca and ^{40}Ca.

B. Incorporation of the Coulomb energy

The predicted binding energies, E_{Bint}, of the WBMB and USD interactions do not include Coulomb contributions, that is, they are calculated for chargeless nucleons. They are also relative to an ^{16}O core. In order to compare to experiment we will add a Coulomb+core correction, i.e.,

$$E_B(\mathrm{SM}) = E_{Bint} + \Delta_c \ , \tag{2}$$

where SM stands for shell model, either USD or WBMB. Chung and Wildenthal[23] and Wildenthal[24] have extracted experimental values for Δ_c in $(1s,0d)$ shell nuclei by comparison of experimental binding energies of isotope chains, analog states, etc. For each Z they considered several isotones near $N \sim Z$ and adopted a common constant Coulomb energy for all other isotopes of charge Z. Experimentally, we know that there is an A dependence of the Coulomb energy for given Z. This A dependence is absorbed—at least partially—into the parameters of the USD interaction in the least-squares fitting process. Since our WBMB interaction is firmly anchored to the USD interaction, we will use the same recipe. A good phenomenological expression for the Chung-Wildenthal Coulomb+core energy for $Z = 9-20$ is

$$\Delta_c(Z) = E_B(^{16}\mathrm{O}) + 18\,247.80 - 950.495 \cdot Z - 162.025 \cdot Z^2 + 45.29\delta_{Z,\mathrm{odd}} \ \mathrm{keV} \ , \tag{3}$$

where $E_B(^{16}\mathrm{O}) = 127\,620$ keV $[\equiv \Delta_c(8)]$. Note that we use the convention that binding energies are positive. Equation (3) represents the Δ_c of Chung and Wildenthal for $Z = 11-20$, $N = 15-20$ with an average (maximum) deviation of 15 (30) keV. The E_B(SM) presented here are obtained from the shell-model predictions using Eqs. (2) and (3).

C. Calculations

The calculations were done on VAX computers with the program OXBASH (Ref. 25) which works in the m scheme but utilizes projected basis vectors which have good J and T. With the computer resources available to us (the principal limitation is the available disk space) we can handle states with J dimensions, $D(J)$, up to $\sim 11\,000$. For larger dimensions, some sort of truncation is necessary as will be explained in Sec. IV. In OXBASH, spuriosity is investigated and often eliminated using the *approximate* method of Gloeckner and Lawson.[26]

III. $0\hbar\omega$ BINDING ENERGIES OF NEUTRON-RICH $Z = 8-20$ NUCLEI

In this section we present predictions for ground-state binding energies calculated in a $0\hbar\omega$ basis. Results are given in Table II. We include some $N \leq 20$ nuclei in Table II because the results are needed to extend the systematics and for weak-coupling calculations which will be considered in Sec. IV. The calculations were done with the normal filling of the shell-model orbits and—with the exception of ^{36}Al, ^{37}Si, and ^{38}P—without truncation. Many nfp spectra other than those listed in Table II have been calculated. These include $1fp$ and some $\geq 2fp$ spectra for $N \leq 20$ nuclei as well as nfp spectra with $n > N-20$ for $N > 20$ nuclei. Some of these spectra are included in Ref. 14. All are available upon request. For $N > 20$, there are no disagreements with experiment for the predicted ground-state J^π of Table II. The disagreements for ^{29,31}Na were one of the first indications of the "island of inversion."[5] Most of the J^π values for the odd A nuclei are those expected from an extreme independent-particle model. Two exceptions are found. For the $Z = 8,10,12$ $N = 23,25$ nuclei, the fp neutrons couple to $\frac{3}{2}^-$ rather than $\frac{7}{2}^-$. This is mostly due to the lower $p_{3/2}-f_{7/2}$ energy gap (as will be apparent from the results presented for effective single-particle energies in Sec. V A) but also is a manifestation of deformation. For the $N = 22$ and 24 Na isotopes the predicted J^π is $\frac{3}{2}^+$ rather than $\frac{5}{2}^+$. This is certainly an effect of prolate deformation. These two effects combine to produce the rather unusual $J^\pi = 0^-$ for ^{34}Na from a $\tilde{j}_p \otimes \tilde{j}_h$ coupling of $\frac{3}{2}^- \otimes \frac{3}{2}^+$.

The ground-state binding energies predicted by the WBMB are compared to experiment via the difference between the WBMB model prediction, E_B(WBMB), and the experimental binding energy, E_B(Exp),

$$\Delta E_B = E_B(\mathrm{WBMB}) - E_B(\mathrm{Exp}) \ . \tag{4}$$

Apart from the Coulomb energy parametrization developed here, $(1s,0d)$ binding energies are given by the USD interaction;[15,24] however, they are replicated by the WBMB interaction and, for simplicity, we shall usually refer to the calculations for all nuclei considered as WBMB predictions. The experimental mass values listed in Table II are obtained from the compilation of Wapstra, Audi, and Hoekstra[39] or the individual literature citations.

TABLE II. Predicted and experimental binding energies for neutron-rich $Z=8$–20 nuclei. All energies are in keV. ΔE_B is prediction–experiment. Unless otherwise referenced, masses are from Ref. 39.

Nucleus	N	J^π WBMB	J^π Experiment[a]	Binding energy WBMB	Binding energy Experiment	ΔE_B WBMB[b]	References or remarks[c]
^{25}O	17	$\frac{3}{2}^+$	unknown	167 899			d
^{26}O	18	0^+	0^+	169 664			
^{27}O	19	$\frac{3}{2}^+$	unknown	167 912			d
^{28}O	20	0^+	0^+	168 879			
^{29}O	21	$\frac{7}{2}^-$	unknown	164 731			d; $\frac{3}{2}^-$, 74 keV
^{30}O	22	0^+	0^+	164 484			d
^{31}O	23	$\frac{3}{2}^-$	unknown	160 218			e; $\frac{7}{2}^-$, 138 keV
^{32}O	24	0^+	0^+	159 610			d
^{33}O	25	$\frac{3}{2}^-$	unknown	155 235			e; $\frac{7}{2}^-$, 321 keV
^{27}F	18	$\frac{5}{2}^+$	unknown	187 524	185 286±700	2238	[40]
^{28}F	19	3^+	unknown	187 082			2^+, 202 keV
^{29}F	20	$\frac{5}{2}^+$	unknown	188 452			
^{30}F	21	6^-	unknown	186 765			d
^{31}F	22	$\frac{5}{2}^+$	unknown	187 134			e, [14]
^{32}F	23	2^-	unknown	184 912			d; 3–4^-, $\leq$267 keV
^{33}F	24	$\frac{5}{2}^+$	unknown	184 813			e
^{34}F	25	4^-	unknown	181 883			d; 2^-, 17 keV
^{28}Ne	18	0^+	0^+	207 726	207 200±317	526	f
^{29}Ne	19	$\frac{3}{2}^+$	unknown	207 597			d
^{30}Ne	20	0^+	0^+	210 126			
^{31}Ne	21	$\frac{7}{2}^-$	unknown	209 183			d, [14]
^{32}Ne	22	0^+	0^+	212 224			e, [14]
^{33}Ne	23	$\frac{3}{2}^-$	unknown	211 077			d; $\frac{5}{2}^-$, 274 keV
^{34}Ne	24	0^+	0^+	212 752			d; g.s. only calculated
^{35}Ne	25	$\frac{3}{2}^-$	unknown	210 497			d; g.s. only calculated
^{29}Na	18	$\frac{5}{2}^+$	$\frac{3}{2}^{(+)}$	223 542	222 818±122	721	f,g; $\frac{3}{2}^+$, 137 keV; [28,29]
^{30}Na	19	2^+	2	224 923	225 374±323	−448	f; 0–3^+, $\leq$301 keV; [28]
^{31}Na	20	$\frac{5}{2}^+$	$(\frac{3}{2})$	228 142	229 585±492	−1439	f,g, [28]
^{32}Na	21	3^-	unknown	228 697	233 128±740	−4431	2–6^-, $\leq$221 keV; [14]
^{33}Na	22	$\frac{3}{2}^+$	unknown	232 205	236 279±1140	−4075	$\frac{5}{2}^+$, 18 keV; [14]
^{34}Na	23	0^-	unknown	233 032			2–4^-, $\leq$424 keV; [14]
^{35}Na	24	$\frac{3}{2}^+$	unknown	235 151			g.s. only calculated
^{30}Mg	18	0^+	0^+	242 062	241 793±210	239	[41]
^{31}Mg	19	$\frac{3}{2}^+$	unknown	243 860	244 221±138	−340	f
^{32}Mg	20	0^+	0^+	248 355	249 696±170	−1341	f
^{33}Mg	21	$\frac{7}{2}^-$	unknown	249 602	251 877±840	−2275	[14,42]
^{34}Mg	22	0^+	0^+	254 488			
^{35}Mg	23	$\frac{3}{2}^-$	unknown	255 362			$\frac{5}{2}$–$\frac{7}{2}^-$, $\leq$254 keV
^{36}Mg	24	0^+	0^+	254 347			g.s. only calculated

TABLE II. (*Continued*).

Nucleus	N	J^π WBMB	J^π Experiment[a]	Binding energy WBMB	Binding energy Experiment	ΔE_B WBMB[b]	References or remarks[c]
^{31}Al	18	$\frac{5}{2}^+$	$\leq\frac{5}{2}^+$	255 352	255 092±70	260	[30]
^{32}Al	19	1^+	1^+	259 193	259 990±138	−797	f; 4^+&2^+, 425&687 keV; [29]
^{33}Al	20	$\frac{5}{2}^+$	unknown	264 940	264 860±126	80	f
^{34}Al	21	4^-	$[4^-]$	267 262	267 506±200	−244	f; $\frac{5}{2}^-$, 2 keV; [31,32]
^{35}Al	22	$\frac{5}{2}^+$	unknown	272 555	272 650±430	−95	[14,42]
^{36}Al	23	4^-	unknown	274 384			truncated; $1-5^-$, ≤377 keV
^{32}Si	18	0^+	0^+	271 373	271 412±1	−39	
^{33}Si	19	$\frac{3}{2}^+$	$\leq\frac{5}{2}^+$	275 701	275 894±16	−193	[33]
^{34}Si	20	0^+	0^+	283 551	283 432±15	119	
^{35}Si	21	$\frac{7}{2}^-$	$[\frac{7}{2}^-]$	286 364	285 906±55	458	[34,35]
^{36}Si	22	0^+	0^+	292 753	292 253±270	500	d, [31]
^{37}Si	23	$\frac{7}{2}^-$	unknown	294 739			truncated; $\frac{3}{2}-\frac{5}{2}^-$, ≤328 keV
^{33}P	18	$\frac{1}{2}^+$	$\frac{1}{2}^+$	281 148	280 958±1	190	
^{34}P	19	1^+	1^+	287 172	287 248±1	−76	
^{35}P	20	$\frac{1}{2}^+$	$\frac{1}{2}^+$	295 860	295 621±2	239	[36]
^{36}P	21	4^-	$[4^-]$	299 611	299 085±13	526	3^-, 169 keV; [31]
^{37}P	22	$\frac{1}{2}^+$	unknown	306 674	305 987±115	687	h, [31]
^{38}P	23	4^-	unknown	309 712	308 407±580	1305	truncated; $1-3^-$, ≤158 keV; [42]
^{36}S	20	0^+	0^+	308 715	308 716±1	1	
^{37}S	21	$\frac{7}{2}^-$	$\frac{7}{2}^-$	313 224	313 019±1	205	[14]
^{38}S	22	0^+	0^+	321 208	321 056±7	152	[14]
^{39}S	23	$\frac{7}{2}^-$	$[\frac{7}{2}^-]$	325 250	325 430±50	−181	$\frac{3}{2}-\frac{5}{2}^-$, ≤203 keV; [37,44]
^{40}S	24	0^+	0^+	332 746	332 857±40	−111	g.s. only; [38]
^{37}Cl	20	$\frac{3}{2}^+$	$\frac{3}{2}^+$	317 242	317 103±1	139	
^{38}Cl	21	2^-	2^-	323 468	323 210±1	258	[14]
^{39}Cl	22	$\frac{3}{2}^+$	$\frac{3}{2}^+$	331 646	331 287±19	359	[14]
^{40}Cl	23	2^-	2^-	337 228	337 085±40	143	[14]
^{38}Ar	20	0^+	0^+	327 297	327 345±1	−48	
^{39}Ar	21	$\frac{7}{2}^-$	$\frac{7}{2}^-$	334 017	333 942±5	75	[14]
^{40}Ar	22	0^+	0^+	343 728	343 812±1	−84	[14]
^{41}Ar	23	$\frac{7}{2}^-$	$\frac{7}{2}^-$	350 006	349 910±1	96	[14]
^{42}Ar	24	0^+	0^+	359 551	359 335±40	216	[14]
^{39}K	20	$\frac{3}{2}^+$	$\frac{3}{2}^+$	333 869	333 726±1	143	
^{40}K	21	4^-	4^-	341 633	341 524±1	109	[14]
^{41}K	22	$\frac{3}{2}^+$	$\frac{3}{2}^+$	351 893	351 620±1	273	[14]
^{42}K	23	2^-	2^-	359 491	359 153±1	338	[14]
^{43}K	24	$\frac{3}{2}^+$	$\frac{3}{2}^+$	369 399	368 797±9	602	[14]
^{40}Ca	20	0^+	0^+	342 149	342 056±1	93	
^{41}Ca	21	$\frac{7}{2}^-$	$\frac{7}{2}^-$	350 514	350 416±1	98	[14]
^{42}Ca	22	0^+	0^+	361 862	361 898±1	−36	[14]
^{43}Ca	23	$\frac{7}{2}^-$	$\frac{7}{2}^-$	370 080	369 830±1	250	[14]
^{44}Ca	24	0^+	0^+	381 243	380 962±1	281	[14]

TABLE II. (*Continued*).

[a]The usual assumption is made that even-even nuclei have 0^+ ground states. The spin-parity assignments in parentheses are most probable values and those in brackets are model-dependent speculations. Unless given by the reference listed in the last column, the spin-parity assignments are from Ref. 27.

[b]For $Z \leq 20$, the WBMB predictions are identical to those of the USD interaction (Refs. 15 and 24) but with our Coulomb+core correction.

[c]If published, the reference for the spectrum is given. The other spectra are available upon request. In some cases it is judged that the excitation energy of an excited state (or states) is not sufficiently higher than the ground state to make a clear prediction as to its spin. In these cases the J^π (or range of J^π) and the excitation energy (or energy range) are given in the form J^π, E_x. Reference numbers are enclosed in square brackets.

[d]The nuclide is one-particle unstable.

[e]The nuclide is two-particle unstable, but not one-particle unstable.

[f]Weighted average of the two or three values reported in Refs. 39, 41, and 42.

[g]The WBMB binding energy prediction is for the predicted J^π.

[h]Weighted average of the two values reported in Refs. 41 and 43. The measurement of Ref. 42 differs 3 standard deviations from this value and is not included.

Figure 2 illustrates ΔE_B for nuclei considered within our model space. Experimental error bars are shown only when they exceed the size of the plotting symbol. An overview of the figure shows very good agreement between calculation and experiment for all the nuclei considered apart from the island of deformation centered at $Z=11$ and $N=21$. The USD interaction was already known to give very good agreement between experimental and calculated binding energies—the root-mean-square deviation between prediction and experiment, ΔE_B(rms), for 440 levels is 185 keV (Ref. 18). For $35 < A < 43$ nuclei with $Z \geq 16$, $N > 20$ the WBMB interaction also produces excellent agreement with ΔE_B(rms)=195 keV for the 18 ground-state binding energies of Table II in the indicated range. If now we include the seven $N > 20$, $Z = 13-15$ nuclei of Table II, ΔE_B(rms) increases to 305 keV: There is an indication that the WBMB overbinds the $Z < 16$ nuclei and we keep this in mind, but note that the predictive power is good compared to the magnitude of the mass anomaly under investigation. A more comprehensive critique of the ability to predict binding energies would be a comparison to known energy levels rather than just ground states. A detailed comparison of this type is made in Ref. 14. It was on this basis, in fact, that the *fp-sd* energy gap was arrived at, as already mentioned (see Sec. II A).[45] The present emphasis is on ground-state binding energies and so we restrict our discussion to them.

It is of interest to compare the predictive powers of the WBMB for nuclear masses to those of semiempirical mass formulas. Möller, Myers, Swiatecki, and Treiner[46] have deduced a nuclear mass formula based on a finite-range droplet model and a folded Yukawa single-particle potential. This model is representative in accuracy of current semiempirical mass formulas and we use it to represent these mass formulas. Figure 3 illustrates the binding energy difference between model and experiment for the isotopes of both S and Mg. Results are shown for the semiempirical mass formula of Möller *et al.*,[46] and for the WBMB. We see that, as expected, the shell-model predictions are in much better agreement with experiment than the mass formula. For the same 25 nuclei in the range $Z=13-20$ for which the WBMB ΔE_B(rms) is 305 keV, Möller *et al.* predict the nuclear mass with an rms deviation of 1410 keV. Moreover we note (i) that the deviations with experiment are such that the semiempirical mass formula cannot be used to uncover the "island of inversion" and (ii) that plots of the two neutron separa-

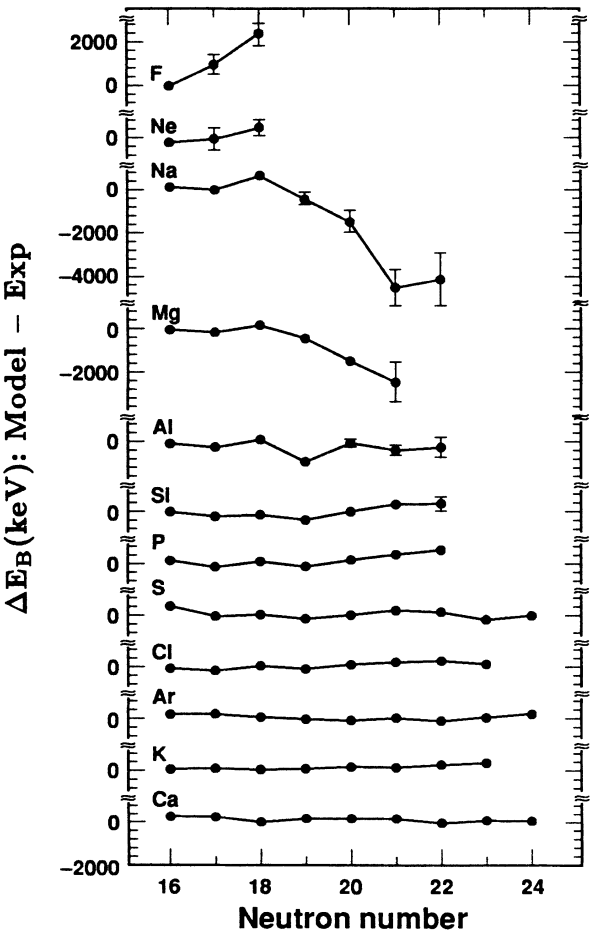

FIG. 2. The ground-state binding energies of *sd* and *sdpf* nuclei compared to experiment. The *sd* shell nuclei are calculated with the USD interaction of Wildenthal (Ref. 15), and the *sdpf* shell nuclei ($N > 20$) are calculated with the WBMB interaction.

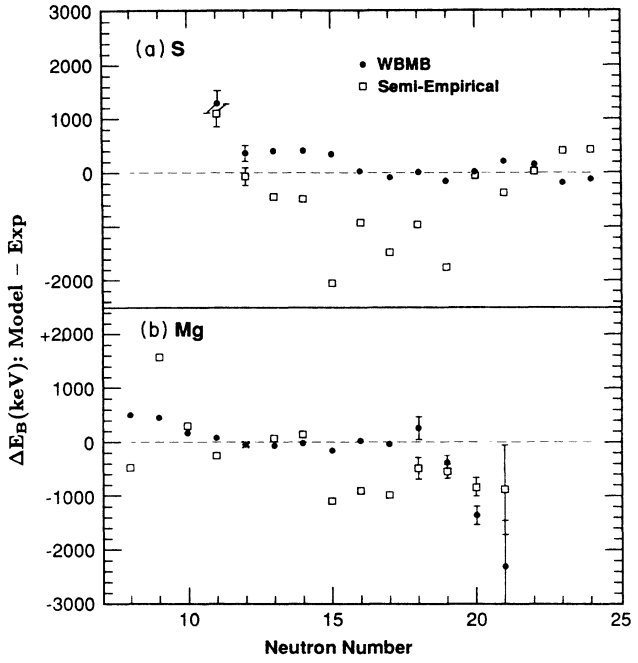

FIG. 3. The ground-state binding energies for the isotopes of sulfur (a) and magnesium (b) compared to the predictions of the WBMB interaction and the semiempirical mass formula of Möller *et al.* (Ref. 46).

tion energy $S(2n)$ vs nuclide can be misleading with respect to the quality of agreement between mass prediction and experiment.

Because of the generally good predictive powers of the WBMB for ground-state binding energies, any systematic departure from agreement with experiment suggests that a nuclear structure effect not included in the model is coming into play. We see from Table II or Fig. 2 that the WBMB interaction does not predict enough binding for $^{31-33}$Na and $^{32-33}$Mg. As discussed in the Introduction, Wildenthal and Chung[5] showed that the USD interaction underpredicts the binding of ^{31}Na and ^{32}Mg, and referred to an "island of inversion." Based on the mass predictions of the WBMB interaction, we see that the "island" includes $^{32-33}$Na and ^{33}Mg as well, as was also found by Poves and Retamosa.[7] We explore through calculation the extent and nature of this "island of inversion" in the next section.

IV. COEXISTING $0\hbar\omega$ AND $2\hbar\omega$ MODEL STATES

A. Delineation of the calculations

As in previous studies[6-8] we neglect excitations of a nucleon through two oscillation shells such as $0p \rightarrow 1p$ or $(1s,0d) \rightarrow (2s,1d,0g)$. We refer to mp-qh (m particle-q hole)$\rightarrow$($m+n$)p-($q+n$)h excitations interchangeably as $n\hbar\omega$ excitations. It is relevant to ask about the binding energy of $N \sim 20$ nuclei for configurations due to promotion of two protons from the $0p$ to the $(1s,0d)$ shell both with and without promotion of two neutrons from the $(1s,0d)$ shell to the $(0f,1p)$ shell. Such states were considered in ^{28}O using the latest version[47] of the Millener-Kurath interaction in $(0p)^{10}(1s,0d)^{14}$ and $(0p)^{10}(1s,0d)^{12}(0f,1p)^2$ model spaces (denoted *psd* and *psdfp* model spaces, respectively). The first calculation involved the full *psd* model space. For the calculation in the *psdfp* model space, the full $(0p)$ and $(0f,1p)$ spaces were used but the $(1s,0d)$ space was truncated to protons in the $d_{5/2}$ orbit and neutron holes in the $d_{3/2}$ orbit only. The 0^+ ground states of these two spaces were found to lie $\sim$14 and $\sim$20 MeV, respectively, above the $(0p)^{12}(1s,0d)^{12}$ ground state. The reason for these high excitations appears to be the large amount of energy lost in promoting the two protons from the $0p$ to the $(1s,0d)$ shell. Thus, it appears that $0p \rightarrow (1s,0d)$ excitation of protons can be neglected from energy considerations. We shall comment further on this question when we discuss the role of single-particle energies on the relative $2\hbar\omega$ and $0\hbar\omega$ energies in Sec. V A. Thus, as in the previous studies, our excitations are limited to $(1s,0d) \rightarrow (0f,1p)$. We should caution that this truncation will lead to spurious center-of-mass motion which might be excessive (and which is not removed by the Gloeckner-Lawson[26] prescription) in some cases; e.g., $1\hbar\omega$ excitations in $Z=8$ and 9 nuclei. Checks have been made and spuriosity is not a problem for the nuclei of main interest to this study.

B. Relative $0\hbar\omega$ and $2\hbar\omega$ binding energies of $Z=8-18$, $N=18-23$ nuclei

1. Dimensions

An appreciation of the dimensions of the matrices involved in the $2\hbar\omega$ calculations for the $A \sim 32$, $N \sim 21$ region can be obtained from Table III which gives $D(J)$ for $Z=8-10$, $N=19-22$ nuclei for both $0\hbar\omega$ and $2\hbar\omega$ states. The dimensions become dramatically higher for $Z=11-14$. Only for $Z=8$ can we handle the $2\hbar\omega$ calculations in the full *sdpf* space for all $N=19-22$ nuclei.

We see from Table III that as a consequence of shell closure, the $N=20$ nuclei have considerably smaller $2\hbar\omega$ dimensions than the $N=19$, 21, and 22 nuclei. Since we are interested in maintaining as complete an *sdpf* model space as possible, we consider the $N=20$ isotones in more detail than the other $N=19-22$ nuclei in the region of interest. The results for $N=20$ also give us a criterion for judging the approximations we adopt later in this paper.

The $Z=8-10$, $N=20$ $2\hbar\omega$ ground states can all be diagonalized in the full *sdpf* space, but $D(J)$ reaches a maximum of 15 003 for $J^\pi=3^+$ for ^{30}Ne so that the complete ^{30}Ne $2\hbar\omega$ spectrum cannot be diagonalized in the full *sdpf* model space. Truncation is also necessary for diagonalization of the $2\hbar\omega$ ground states of ^{31}Na and ^{32}Mg since these have $D(J)$ values of $D(\frac{3}{2}^+)=34\,525$, and $D(0^+)=20\,702$, respectively. Thus, we now turn to a consideration of truncation schemes before continuing the discussion of the $N=20$ isotones.

TABLE III. J dimensions of the $0\hbar\omega$ (upper) and $2\hbar\omega$ (lower) $sdpf$ model spaces for the $N=19$–22, $Z=8$–10 isotopes. The J^π of the most bound state of the model space is given. Those in parentheses are assumed.

$Z\backslash N=$	19	20	21	22
8	1 $\frac{3}{2}^+$	1 0^+	1 $\frac{7}{2}^-$	4 0^+
	686 $\frac{3}{2}^+$	80 0^+	1059 $\frac{3}{2}^-$	1042 0^+
9	6 3^+	1 $\frac{5}{2}^+$	1 6^-	63 $\frac{5}{2}^+$
	9272 (3^+)	2947 $\frac{5}{2}^+$	10 323[a] (6^-)	51 976 $(\frac{5}{2}^+)$
10	29 $\frac{3}{2}^+$	3 0^+	38 $\frac{7}{2}^-$	80 0^+
	28 584[a] $(\frac{3}{2}^+)$	3 271 0^+	73 024[a] $(\frac{7}{2}^-)$	49 906[a] 0^+

[a]For $sd\rightarrow fp$ neutron excitations only.

2. *Truncation schemes for N=20*

We shall consider first the effect of limiting the $sd\rightarrow fp$ excitations to neutrons only, truncation $T(N)$. We then consider three further truncations, all of which also restrict the $sd\rightarrow fp$ excitations to neutrons. These we refer to as $T(f_{7/2}p_{3/2})$, $T(d_{3/2}f_{7/2}p_{3/2})$, and $T(1)$. All three of these truncations allow the full sd shell for protons. $T(f_{7/2}p_{3/2})$ allows the full sd shell for neutrons but restricts the fp shell to the $f_{7/2}$ and $p_{3/2}$ orbits. $T(d_{3/2}f_{7/2}p_{3/2})$ allow neutron excitations from the $d_{3/2}$ orbit to the $f_{7/2}$ and $p_{3/2}$ orbits only. The truncation $T(1)$ is most succinctly explained in terms of partitions. A partition $\mathcal{P}$ is a specific combination of active orbits. Thus, a particular wave function will be composed, in general, of many partitions:

$$\mathcal{P}=[p(d_{5/2}),p(d_{3/2}),p(s_{1/2})|n(d_{5/2}),n(d_{3/2}),n(s_{1/2});n(f_{7/2}),n(f_{5/2}),n(p_{3/2}),n(p_{1/2})]\ , \tag{5a}$$

where $p(j)$ and $n(j)$ are the number of protons and neutrons, respectively, in a particular orbit j. The $p(j)$ for the fp shell are omitted since we restrict proton occupancy to the sd shell in all truncations. Another useful concept is the mean partition $\bar{\mathcal{P}}(J_k^\pi)$ given by

$$\bar{\mathcal{P}}(J_k^\pi)=[\bar{p}(d_{5/2}),\bar{p}(d_{3/2}),\bar{p}(s_{1/2})|\bar{n}(d_{5/2}),\bar{n}(d_{3/2}),\bar{n}(s_{1/2});\bar{n}(f_{7/2}),\bar{n}(f_{5/2}),\bar{n}(p_{3/2}),\bar{n}(p_{1/2})]\ , \tag{5b}$$

where $\bar{p}(j)$ and $\bar{n}(j)$ are the mean number of protons and neutrons, respectively, in orbit j for the state J_k^π. For $T(1)$, all possible sd proton partitions are allowed and the allowable neutron partitions are

$$[4\text{–}6,2\text{–}4,0\text{–}2;2,0,0,0]+[6,2\text{–}4,0\text{–}2;0\text{–}1,0,0\text{–}2,0]+[6,2,2;r_f,0\text{–}2,r_p,0\text{–}2];\quad r_f+r_p<2\ . \tag{6}$$

Results for the four truncation schemes are compared to each other and to those for the full $sdpf$ model space in Table IV. The $N=20$ isotones considered are those for which calculation in the full model space is possible; namely, ^{28}O, ^{29}F, and ^{30}Ne. We include ^{38}Ar to illustrate the effect of nearly filling the sd proton shell. The last column of Table IV lists the percentage of the wave function in the full $2\hbar\omega$ calculation which resides in the partitions contained in the indicated truncation. This percentage is a good representation of the overlap of the two wave functions. Thus, the accuracy of a given truncation can be gauged by the deviation of the binding energy from the "full" result or from the degree of overlap shown in the last column. Note that it is a rigorous property of shell-model calculations that the effect of truncation is always to render a ground state less bound. From Table IV we see that the exclusion of proton excitations has a very small effect for the three $Z\leq 10$ cases, and even for ^{38}Ar the $2\hbar\omega$ excitations are overwhelmingly of neutrons. A second point of interest is that $T(1)$—although smaller in dimensions than $T(f_{7/2}p_{3/2})$—is an appreciably better approximation to our touchstone of the full $sdpf$ model space. We note two strong regularities for the four nuclei of Table IV. First, the dimensions of $T(1)$ are all $\sim$24% of those for $T(N)$. Second, the $T(1)$ contribution to the $T(N)$ wave function is remarkably constant at $\sim$97%. The major change between ^{30}Ne and ^{38}Ar occurs in the $T(N)$ contribution to the full $2\hbar\omega$ wave function, and, as already remarked, that change is quite small. $T(1)$ can be used to calculate the $2\hbar\omega$ ground-state binding energies of ^{31}Na, ^{32}Mg, ^{34}Si, ^{36}S, and ^{37}Cl. The nuclei ^{33}Al$(\frac{5}{2}^+)$ and ^{35}P$(\frac{1}{2}^+)$ have $D(J)$ in the $T(1)$ truncation of 32 126, and 13 315, respectively, and thus are beyond our capabilities. We derive the small truncation correction, $\Delta(T1)$ from the results of Table IV. For $A\leq 34$ the $d_{5/2}$ orbit is at the Fermi surface and we expect little change in $\Delta(T1)$ from the $A=28$–30 cases shown. These have a weighted average of 594(37) keV and this correction is used for ^{31}Na, ^{32}Mg, and ^{34}Si. For $35\leq A\leq 38$ we expect some increase in $\Delta(T1)$ since

TABLE IV. Comparison of binding energies of the $N=20$ isotones for $Z=8-10$ and 18 calculated with various truncation schemes. All model spaces are $2\hbar\omega$ except that labeled $0\hbar\omega$. The calculated $0\hbar\omega$ and $2\hbar\omega$ ^{29}F ground states are both $J^\pi=\frac{5}{2}^+$. Coulomb energies are not included.

Nucleus	Z	N	T_z	Model space	J dimensions $J=0$ or $\frac{1}{2}$	$J=4$ or $\frac{5}{2}$	E_{Bint} (keV) Shell model	% in full $2\hbar\omega$
^{28}O	8	20	6	$0\hbar\omega$	1	0	41 259	
				Full($2\hbar\omega$)	80	271	38 303	100.00
				$T(N)$	80	271	38 303	100.00
				$T(1)$	23	68	37 743	97.44
				$T(f_{7/2}p_{3/2})$	27	90	37 191	90.38
				$T(d_{3/2}f_{7/2}p_{3/2})$	5	10	36 080	84.10
^{29}F	9	20	$\frac{11}{2}$	$0\hbar\omega$	1	1	64 217	
				Full($2\hbar\omega$)	1323	2947	62 879	100.00
				$T(N)$	1291	2882	62 824	99.95
				$T(1)$	306	689	62 325	97.07
				$T(f_{7/2}p_{3/2})$	387	894	61 820	90.01
				$T(d_{3/2}f_{7/2}p_{3/2})$	43	96	60 561	82.44
^{30}Ne	10	20	5	$0\hbar\omega$	3	2	89 966	
				Full($2\hbar\omega$)	3271	14 758	90 754	100.00
				$T(N)$	3118	14 162	90 732	99.90
				$T(1)$	763	3449	90 085	96.28
				$T(f_{7/2}p_{3/2})$	968	4622	89 503	88.92
				$T(d_{3/2}f_{7/2}p_{3/2})$	114	474	87 887	79.84
^{38}Ar	18	20	1	$0\hbar\omega$	3	2	251 035	
				Full($2\hbar\omega$)	4737	21 636	248 334	100.00
				$T(N)$	3118	14 162	248 092	98.08
				$T(1)$	763	3449	247 571	95.15

the active protons are somewhat less bound. For these $N=20$ isotones we obtain the correction from a linear interpolation between 594 keV at $A=34$ and 763 keV at $A=38$.

One further truncation was used in this study. For the $N=23$, $Z=13-15$ isotones the J dimensions were just beyond our resources; $D(4^-)=13\,854$ for ^{36}Al and ^{38}P and $D(\frac{7}{2}^-)=16\,102$ for ^{37}Si. The truncation used was to take only the most bound proton partition for those neutron partitions with $n(f_{7/2})+n(p_{3/2})<2$. This decreased the J dimensions to $D(4^-)=8719$ for ^{36}Al, 8690 for ^{38}P, and $D(\frac{7}{2}^-)=10\,011$ for ^{37}S. The decrease in binding due to this truncation was estimated by comparing the results to the full calculation for the low and high spin states for which the full calculation was possible. The decrease was only $\sim$200 keV and so could be estimated with no appreciable uncertainty.

3. *A weak-coupling approximation*

We have found that the predicted binding of $n\hbar\omega$ excitations are well reproduced in a simple weak-coupling model. Thus the excitation energy of the lowest 2p-2h ($2\hbar\omega$) state relative to the 0p-0h ground state of an $N=20$ nucleus in our weak-coupling approximation is

$$E_x^{(wc)}(N=20;2\hbar\omega)=2\cdot E_B(20)-[E_B(22)+E_B(18)] -2\cdot 2\cdot C\ , \quad (7)$$

where all the $E_B(N)$ are predictions for isotopes of the atomic number Z. The generalization of Eq. (7) to $n\hbar\omega$ excitations of the mp-$(m+20-N)$h configuration is

$$E_x^{(wc)}(N;n\hbar\omega)=[E_B(N)+E_B(20)] -[E_B(20+m+n)+E_B(N-m-n)] -(m+n)(m+n+20-N)C\ , \quad (8)$$

where, for excitation of $0\hbar\omega$ states, $m=0$ for $N\leq 20$ and $m=N-20$ for $N>20$.

Many examples of the weak-coupling model have been discussed for nuclei around ^{16}O and ^{40}Ca where the residual interaction between particles and holes has an isospin dependence.[48] In our case the form of the particle-hole interaction is much simpler since only neutrons are presumed to be excited. The motivation for the weak-coupling formula is as follows. Consider, as an example, the $N=19$ nucleus ^{31}Mg which has a $0\hbar\omega$ configuration of one neutron hole (1h) in the *sd* shell relative to the $N=20$ neutron closed shell. The $n\hbar\omega$ configuration is then np-$(n+1)$h with n neutron particles in the *fp* shell and $n+1$ neutron holes in the *sd* shell. In analogy with the expression for 1p-1h states in closed shell nuclei, the energy of this $n\hbar\omega$ configuration relative to the $N=20$ closed shell is

$$E(N=19;n\hbar\omega)-E(N=20;0\hbar\omega)$$
$$=e(np)-e[(n+1)h]-n(n+1)C\ , \quad (9)$$

where we write $E(N;n\hbar\omega)$ for $-E_B(N;n\hbar\omega)$ so that the normal physical meaning for binding energies (negative) is retained in this discussion. The term $n(n+1)C$ takes into account the average 1p-1h interaction C between neutrons. The particle energy is given by $e(np)=E(N=20+n;0\hbar\omega)-E(N=20;0\hbar\omega)$ and the hole energy is given by $e[(n+1)\text{h}]=E(N=20;0\hbar\omega)-E(N=19-n;0\hbar\omega)$. Combining these results we obtain

$$E_x^{(wc)}(N=19;n\hbar\omega)=E(N=19-n;0\hbar\omega)+E(N=20+n;0\hbar\omega)-E(N=20;0\hbar\omega)-E(N=19;0\hbar\omega)-n(n+1)C\ . \quad (10)$$

This result can be generalized to the form of Eq. (8). The weak-coupling model can be presumed to be useful if the dominant interactions are taken into account by the $E_B(N;0hw)$ and the residual interaction C is weak. This appears to be true in our case. There is the additional assumption that the energies and structure of the $e(np)$ and $e[(n+1)\text{h}]$ configurations do not change much when they are coupled together.

As stated above, the energy C represents the interaction between a single fp neutron and a single sd neutron hole. It was evaluated by comparison to explicit model calculations for those cases which were done. Thus we use $C=143$ keV for $Z=8$ and $C=240+10\cdot(Z-9)$ keV otherwise. It is perhaps not surprising that this weak-coupling approximation is a very good one for $n\hbar\omega$ excitations with both n and N even since in this case the fp neutrons and sd neutron holes can each be expected to couple to 0^+ to a good approximation. We also find it to be good for $n\hbar\omega$ excitations which result in an odd number of fp neutrons coupled to $\tilde{j}_p$ and sd neutron holes coupled to $\tilde{j}_h$. The reason for this is easy to see: The multiplet formed by $\tilde{j}_p\otimes\tilde{j}_h$ is closely spaced due to the small magnitude of the $T=1$ particle-hole interaction and thus the binding energy of the lowest state of this multiplet is not much different from the binding energy of the multiplet's centroid; i.e., the neglect of the j dependence of the residual interaction between the neutron particles and holes is not too serious.

4. Results for $2\hbar\omega$ excitations

Our results for the relative binding energies, $E_x(2\hbar\omega)$, of the ground states of the lowest allowed configuration and the $2\hbar\omega$ excitation of that configuration are collected in Fig. 4. The result of the full WBMB calculation, F, or of truncation $T(1)$, T, are given when possible; but most entries are for the weak-coupling prediction, W. A comparison of the F and/or T results to the W entries for those cases for which the full or truncated calculation was possible illustrates that weak-coupling gives an excellent estimate of the relative binding energies.

In addition to the results of Fig. 4, predictions for the $E_x(2\hbar\omega)$ of the $N=20$ nucleus $^{36}\text{S}(0^+)$ are 3009 keV in truncation $T(1)$ and 3146 keV in weak-coupling as opposed to 3346 keV for the experimental excitation energy of the 0_2^+ state which is presumably mostly $2\hbar\omega$ in character. Likewise we find for $^{37}\text{Cl}(\frac{3}{2}^+)$, 3091 keV in truncation $T(1)$ and 3195 keV in weak-coupling, while the first predominantly $2\hbar\omega$ state has been identified[13] at 3708 keV. For $^{38}\text{Ar}(0^+)$ the $2\hbar\omega$ prediction is 2701 keV for the full WBMB model space and this result was used to calibrate the weak-coupling parameter C of Eqs. (7) and (8). The ^{38}Ar 0_2^+ state—presumably predominantly $2\hbar\omega$—lies at 3377 keV. We see that the weak-coupling approximation does an excellent job of reproducing the WBMB predictions for all $N=20$ nuclei considered from $Z=8$ to 17; while all predictions underestimate somewhat the separation between the $0\hbar\omega$ and $2\hbar\omega$ states as expected since the interaction between them is neglected.

A study of Fig. 4 reveals a systematic behavior for $E_x(2\hbar\omega)$. It is negative for $Z=10$–12, $N=20$–22, has its lowest value for ^{32}Na, and displays a parabolic dependence on N, Z, or T about ^{32}Na. It may also be negative for $N=23$, $Z=11$ and/or 12, but a trend of increasing $E_x(2\hbar\omega)$ with N for $N>21$ is indicated by the $Z=8$–10 entries. We shall discuss these results in detail in Sec. V B, but first we consider the binding energies of non-normal parity configurations.

5. Results for $1\hbar\omega$ and $3\hbar\omega$ excitations

Since so much energy is gained by promoting two neutrons from the (s,d) shell to the (f,p) shell it is natural to inquire as to the effect of $1\hbar\omega$ and $3\hbar\omega$ excitations, especially in odd N nuclei. Our predictions for $E_x(1\hbar\omega)$ and $E_x(3\hbar\omega)$ are given in Fig. 5. It is seen that indeed the $N=19$, 21, and 23 isotopes of $Z=10$–12 nuclei show very small values of $E_x(1\hbar\omega)$ and for the $N=21$ isotope of Al it even has a negative value. There is a sharp difference between the relative results for the $1\hbar\omega$ and $3\hbar\omega$ spaces versus those for $0\hbar\omega$ and $2\hbar\omega$; namely, we predict that $E_x(1\hbar\omega)$ is always less than $E_x(3\hbar\omega)$. This behavior will be discussed in Sec. V A. From a comparison of Figs. 4 and 5 we conclude that there is strong competition between the $1\hbar\omega$ and $2\hbar\omega$ configurations for the ground state of the $N=19$, 21, and 23 isotopes of the $Z=10$–12 nuclei. Assuming that the increased binding due to the interaction between the $\Delta\hbar\omega=2$ ground states is approximately equal for the two cases, our calculations indicate a quite small difference in the $2\hbar\omega$ and $1\hbar\omega$ energies in several cases. Therefore, we expect both positive and negative parity states at low excitations and the parity of the ground states of these nuclei is an interesting experimental question. For the Ne isotopes there is no available experimental evidence. The β^- decay of the $A=27$–34 Na and Mg isotopes was studied by Guillemaud-Mueller *et al.*[29] while the decays of ^{30}Na and ^{31}Na were recently studied by Baumann *et al.*[49,50] We

now consider information found or reviewed in these studies.

6. *Bearing of β^- decay on the J^π of $N=19$ nuclei*

^{30}Na. For this nucleus—with a known spin of $J=2$—we predict that the $0\hbar\omega$ ground state lies below the $2\hbar\omega(2fp)$ ground state and thus the predicted J^π of the lowest-lying even-parity state is that of the $0\hbar\omega$ configuration, namely 2^+ (Refs. 5 and 24). For the $1\hbar\omega$ model space we predict a low-lying $J=2-5$ quartet with the 2^- state only 74 keV above the 3^- ground state. Thus both the $0\hbar\omega$ and $1\hbar\omega(1fp)$ spin predictions are consistent with $J=2$. Guillemaud-Mueller interpreted their observations to give no significant β^- branch to the 0^+ ^{30}Mg ground state and a logft value of 5.6 for the decay to a 2_1^+ (assumed) state at 1483 keV. Baumann *et al.*[49] assumed no ground-state feeding and obtained a logft of 5.8 for the decay to the 1483-keV level. If correct, this latter decay rules strongly against the 2^- possibility for ^{30}Na but does not rule it out entirely since first-forbidden $\Delta J=0$ transitions of this strength have been observed.[51]

^{31}Mg. The relatively strong β^- branching to low-lying states of ^{31}Al—for which even parity is demanded by its β decay[29]—rules strongly against an odd-parity assign-

Z/N	18	19	20	21	22	23
15	^{33}P +4839:W	^{34}P +3781:W	^{35}P +2698:W	^{36}P +2811:W	^{37}P *D(1/2)* **18823*	^{38}P *D(4$^-$)* *149590*
14	^{32}Si +4134:W	^{33}Si +2716:W	^{34}Si +1816:W +1554:T	^{35}Si +2063:W	^{36}Si +2261:W	^{37}Si *D(7/2)* *169606*
13	^{31}Al +3396:W	^{32}Al +2214:W	^{33}Al +854:W	^{34}Al +786:W	^{35}Al *D(5/2)* **46116*	^{36}Al *D(4$^-$)* *149590*
12	^{30}Mg +2104:W	^{31}Mg +780:W	^{32}Mg − 926:W −966:T	^{33}Mg −1090:W	^{34}Mg − 685:W	^{35}Mg *D(3/2)* **62787*
11	^{29}Na +2317:W	^{30}Na +776:W	^{31}Na −502:W −764:T	^{32}Na −1295:W	^{33}Na − 427:W	^{34}Na *D(4$^-$)** **44735*
10	^{28}Ne +1843:W	^{29}Ne +609:W	^{30}Ne − 698:W − 788:F	^{31}Ne − 891:W	^{32}Ne − 128:W	^{33}Ne + 480:W
9	^{27}F +3273:W	^{28}F +2110:W +2251:F	^{29}F +1286:W +1338:F	^{30}F +1444:W	^{31}F +1329:W	^{32}F +1557:W
8	^{26}O +4246:W +4495:F	^{27}O +3550:W +3568:F	^{28}O +3038:W +2956:F	^{29}O +2870:W +2904:F	^{30}O +2945:W +2905:F	^{31}O +2768:W

FIG. 4. Neutron-rich nuclei in the $A=32$ region. The listed numbers are the predicted excitation energies (in keV) of the $2\hbar\omega$ ground state relative to the $0\hbar\omega$ ground state, $E_x(2\hbar\omega)$. The symbols denote weak coupling, W, the full WBMB model space, F, and the truncation $T(1)$ with the correction $\Delta(T1)$, T. We label the excitation energies beyond our computational resources with asterisks and, for these cases, show the J dimension of the $N+2$ isotope necessary to provide the weak-coupling (W) prediction. The magic numbers $Z=8$ and $N=20$ are emphasized with double lines.

ment to the ^{31}Mg ground state for which the $0\hbar\omega$ and $1\hbar\omega(1fp)$ predictions are $J^\pi=\frac{3}{2}^+$ and $\frac{7}{2}^-$ (from weak coupling), respectively. Information on ^{31}Mg also comes from the decay of ^{31}Na. ^{31}Na has a most probable $J=\frac{3}{2}$ ground state and since $N=20$ we clearly expect a $\frac{3}{2}^+$ assignment. Baumann *et al.*[50] reported a branch to the ^{31}Mg ground state with $\log ft=4.9$. This is further evidence for an even-parity assignment to the ^{31}Mg ground state. Baumann *et al.* reported the presence of five excited states below 2 MeV in ^{31}Mg, all with β^- feedings from ^{31}Na corresponding to $\log ft \geq 5.9$. These results are consistent with our predictions concerning the commencement of odd-parity states at a low excitation energy. Baumann *et al.* observed a first-excited state at 50 keV with a $\log ft$ of 6.0 and a meanlife of 23 ns. This latter γ decay is fast enough so that it must be dipole. Our results would favor odd parity for this excited state since the first $0\hbar\omega$ excited state of $J^\pi=\frac{5}{2}^+$ is predicted by the USD at 1550 keV. If the 50-keV state does have odd parity, then a $\frac{3}{2}^-$ assignment would be indicated since only $\Delta J=0$ first-forbidden decays are observed with such low values of $\log ft$.[51]

^{32}Al. The ground state has been assigned $J^\pi=1^+$ from its β^- decay.[29]

7. *Bearing of β^- decay on the J^π of $N=21$ nuclei*

^{32}Na. The $0\hbar\omega(1fp)$ spectrum of ^{32}Na is characterized by a low-lying 2–6 quintet with a 3^- state only 34 and 78 keV below 2^- and 5^- levels, respectively. The $2\hbar\omega(3fp)$

	18	19	20	21	22	23
15	^{33}P +5720:W *****:F *****:3	^{34}P +1673:W *****:F *****:3	^{35}P +4637:W +4290:F +8531:3	^{36}P +1025:W *****:F *****:3	^{37}P +4750:W *****:F *****:3	^{38}P *****:W *****:F *****:3
14	^{32}Si +5647:W *****:F *****:3	^{33}Si + 935:W *****:F *****:3	^{34}Si +4747:W +4227:F +7710:3	^{35}Si + 881:W *****:F +4042:3	^{36}Si +4994:W *****:F *****:3	^{37}Si +1079:W *****:F *****:3
13	^{31}Al +4505:W *****:F *****:3	^{32}Al + 959:W *****:F *****:3	^{33}Al +3145:W +3086:F +5291:3	^{34}Al − 105:W *****:F *****:3	^{35}Al +3077:W *****:F *****:3	^{36}Al *****:W *****:F *****:3
12	^{30}Mg +4678:W *****:F +8024:3	^{31}Mg + 8:W *****:F +1948:3	^{32}Mg +2972:W +2484:F +3588:3	^{33}Mg − 934:W − 729:F + 87:3	^{34}Mg +2808:W *****:F *****:3	^{35}Mg − 529:W *****:F *****;3
11	^{29}Na +3682:W *****:F +6142:3	^{30}Na + 306:W − 87:F +1830:3	^{31}Na +2404:W +2083:F +2387:3	^{32}Na − 808:W −1347:F + 43:3	^{33}Na +1611:W *****:F *****:3	^{34}Na + 60:W *****:F *****:3
10	^{28}Ne +4426:W +3939:F +7108:3	^{29}Ne + 211:W + 123:F +1861:3	^{30}Ne +3119:W +2666:F +3535:3	^{31}Ne − 909:W −1192:F + 270:3	^{32}Ne +2926:W *****:F +4713:3	^{33}Ne − 146:W *****:F +2371:3
9	^{27}F +3538:W +3821:F +8567:3	^{28}F + 662:W + 687:F +4093:3	^{29}F +2714:W +2721:F +4982:3	^{30}F + 624:W + 630:F +2777:3	^{31}F +2872:W +2780:F +5253:3	^{32}F + 509:W *****:F +2887:3
8	^{26}O + 5480:W + 4808:F +11488:3	^{27}O +2110:W +2015:F +6188:3	^{28}O +4972:W +4255:F +8354:3	^{29}O + 928:W + 833:F +4383:3	^{30}O +4804:W +4020:F +8084:3	^{31}O +1003:W + 878:F +4408:3
Z/N						

FIG. 5. Neutron-rich nuclei in the $A=32$ region. The top two listed numbers are the $E_x(1\hbar\omega)$ in keV for weak coupling, *W*, and the full WBMB model space, *F*. The bottom number is $E_x(3\hbar\omega)$ for weak coupling. We label the excitation energies beyond our computational resources with asterisks. The magic numbers $Z=8$ and $N=20$ are emphasized with double lines.

spectrum—for which we predict a ground state 1295 keV lower than that of $0\hbar\omega$—was not directly calculable, but the weak-coupling prediction from our calculation for ^{34}Na is for a 0^- ground state with 3^-, 2^-, and 4^- states at 73, 329, and 424 keV, respectively. The β^- results for ^{32}Na decay are consistent with an odd-parity ^{32}Na ground state since the lowest states in ^{32}Mg to which decays are observed are at 2859 and 3037 keV. These energies are in not bad agreement with our expectations for the excitation energies of the lowest-lying odd-parity states in ^{32}Mg as can be deduced from Figs. 4 and 5. The $1\hbar\omega(2fp)$ spectrum calculated for ^{32}Na is—like the $2\hbar\omega$ spectrum—rather unusual. We predict a 0^+ ground state followed by 2^+, 1^+, and 3^- states at 224, 263, and 408 keV. These states arise primarily from the coupling $\tilde{j}_p \otimes \tilde{j}_n$ with both $\tilde{j}_p$ and $\tilde{j}_n$ equal to $\frac{3}{2}$ as found for the even N Na isotopes and the $N=23$ Ne and Mg nuclei (see Sec. III A). The ^{32}Na β^- results are also consistent with a $1\hbar\omega(2fp)$ 0^- ^{32}Na ground state; i.e., decay to the 0^+ ^{32}Mg ground state would be isospin forbidden and decay to the 2_1^+ state would be $\Delta J=2$ so that the major decays should be to 1^+ states for which commencement at 2859 keV in ^{32}Mg seems reasonable.

^{33}Mg. There is not enough information on ^{33}Mg to reach any conclusions regarding the J^π of its ground state. We note that, like ^{32}Na, we predict a very close competition between $1\hbar\omega(2fp)$ and $2\hbar\omega(3fp)$.

^{34}Al. Recent experimental results for ^{34}Al decay[32] are in excellent accord with the $0\hbar\omega(1fp)$ prediction[31] of 4^- for the ^{34}Al ground state and an odd-parity $1\hbar\omega(1fp)$ spectrum commencing at $\sim$4.2 MeV in ^{34}Si.

8. Bearing of β^- decay on the J^π of $N=19$ and 21 nuclei: summary

We conclude that the $N=19$ isotopes most likely all have normal parity. We have no evidence for a non-normal parity ground state in the $N=21$ nuclei in question, but ^{32}Na and ^{33}Mg remain as definite possibilities. As regards other odd N nuclei, there is not enough information available on the $Z=11$–13, $N\geq 23$ to draw any conclusions at the present time.

TABLE V. Calculated strengths of the $2_1^+ \rightarrow 0_1^+$ (even A) and $\frac{9}{2}_1^+ \rightarrow \frac{5}{2}_1^+$ (odd A) transitions for the $A=28$–32 $N=20$ isotones. The transitions strengths are in Weisskopf units and are calculated with $\delta e_p = \delta e_n = 0.35e$ in truncation $T(d_{3/2}f_{7/2}p_{3/2})$.

A	Z	$B(E2)$
28	8	0.86
29	9	1.89
30	10	7.26
31	11	8.07
32	12	11.35

9. E2 observables: How deformed are the $2\hbar\omega$ states?

Some trends found for $E2$ rates between the $2\hbar\omega$ states are shown in Tables V and VI. The $E2$ observables were calculated with harmonic-oscillator radial wave functions with an oscillator length $b=(41.467/\hbar\omega)^{1/2}$ fm with $\hbar\omega = 45A^{-1/3} - 25A^{-2/3}$. This gives a calculated rms charge radius of 3.10 fm for ^{31}Na in good agreement with the measured value of 3.12 fm (Ref. 52). Table V illustrates that the $B(E2)$ values increase systematically with A. The $B(E2)$ and $Q(E2)$ shown for ^{30}Ne in Table VI are representative of those for the other nuclei. A breakdown of the contributions to the $E2$ matrix element is informative. Surprisingly, the $\pi s_{1/2}$ and $\pi d_{3/2}$ orbits contribute 56% of the π part of the $2_1^+ \rightarrow 0_1^+$ matrix element. Therefore, in our model space, at least, it is not a good approximation to confine the protons to the $d_{5/2}$ orbit when studying $E2$ properties.[53] Typically, the $\nu f_{5/2}$ and $\nu p_{1/2}$ orbits contribute 10–15 % to the $2_1^+ \rightarrow 0_1^+$ matrix elements; these orbits can be omitted without distorting the $B(E2)$ results unduly. This can be seen in Table VI—restricting the fp neutrons to the $f_{7/2}p_{3/2}$ orbits has little effect on the transition rates. Thus the $T(f_{7/2}p_{3/2})$ truncation is, indeed, an adequate model space for studying the collectivity in the $2\hbar\omega$ states. In truncation $T(1)$, the $\nu s_{1/2}$ and $\nu d_{5/2}$ orbits contribute 5–10 % to the $2_1^+ \rightarrow 0_1^+$ matrix element. For

TABLE VI. Excitation energies, $E_x(J_i^\pi)$, quadrupole moments, $Q(E2;J_i^\pi)$, and $E2$ transition strengths, $B(E2)=[A\cdot e_p + B\cdot e_n]^2$ for the $2\hbar\omega(2fp)$ band of ^{30}Ne. The E_x are in keV, the $Q(E2)$ are in e fm^2, and the $B(E2)$ are in Weisskopf units. (For $A=30$ and 32 one Weisskopf unit = 5.54 and 6.04 e^2fm^4, respectively.) All quantities are from truncation $T(1)$ except for the $B(E2)$ in the last three columns which are from the $T(f_{7/2}p_{3/2})$ and $T(d_{3/2}f_{7/2}p_{3/2})$ truncations for ^{30}Ne and the full $0\hbar\omega(2fp)$ model space for ^{32}Ne, respectively. The $B(E2)$ and $Q(E2;J_i^\pi)$ are calculated with $\delta e_p = \delta e_n = 0.35e$.

			^{30}Ne				^{32}Ne
$J_i^\pi \rightarrow J_f^\pi$	$E_x(J_i^\pi)$	$Q(E2;J_i^\pi)$	A	B	$B(E2)$	$B(E2)^a$	$B(E2)^b$	$B(E2)^c$
$2^+ \rightarrow 0^+$	1055	−10.78	3.55	6.94	9.42	9.39	7.26	7.92
$4^+ \rightarrow 2^+$	2213	−15.26	4.06	7.92	12.28	12.16	9.38	10.28
$6^+ \rightarrow 4^+$	3526	−17.05	3.84	7.64	11.13	11.77	8.90	8.81
$8^+ \rightarrow 6^+$	5231	−16.46	4.15	6.66	11.36	11.41	9.89	8.27
$10^+ \rightarrow 8^+$	6769	−17.93	3.37	5.40	7.48	7.56	7.26	4.73
$12^+ \rightarrow 10^+$	9851	−15.74	1.63	4.39	2.52	2.64	3.00	
$14^+ \rightarrow 12^+$	17310	−8.42	0.55	2.04	0.38	0.46		

[a]Truncation $T(f_{7/2}p_{3/2})$.
[b]Truncation $T(d_{3/2}f_{7/2}p_{3/2})$.
[c]$0\hbar\omega(2fp)$.

$T(d_{3/2}f_{7/2}p_{3/2})$, which omits these two orbits, $\delta e_p=\delta e_n=0.45$ reproduces the ^{30}Ne $2_1^+\rightarrow 0_1^+$ strength of 9.42 Wu found for the $T(1)$ truncation with $\delta e_p=\delta e_n=0.35$. The effect of the increased truncation on $E2$ rates is small and regular; however, as we now discuss, the effect of this truncation on the $Q(E2)$ is drastic.

Results for quadrupole moments are given in Tables VI and VII. From Table VI we see that the $Q(E2)$ for ^{30}Ne have the expected sign for prolate deformation and, like the $B(E2)$, vary regularly. In Table VII we see that, unlike the case for $B(E2)$ values, truncation $T(d_{3/2}f_{7/2}p_{3/2})$ gives quite different results than the full WBMB calculation—which is well represented by truncation $T(1)$. Upon examination it is found that the restriction of the neutron holes to the $d_{3/2}$ orbit is the problem; truncation $T(f_{7/2}p_{3/2})$ gives acceptable results. In $T(1)$, the contributions of the various orbits to $Q(E2)$ are completely coherent (except for a small $\nu d_{3/2}\leftrightarrow s_{1/2}$ term) while in $T(d_{3/2}f_{7/2}p_{3/2})$ the main terms, $\pi d_{5/2}\rightarrow d_{5/2}$ and $\nu f_{7/2}\rightarrow f_{7/2}$, are out of phase with the rest. We conclude that in our model space, restriction of neutron holes to the $d_{3/2}$ orbit alone does not allow an adequate approximation to the collectivity manifest in the full model space. It is interesting that this is apparent from the $Q(E2)$ but not the $B(E2)$. Unfortunately, there are not likely to be any experimental measurements of these $Q(E2)$.

The success of the weak-coupling approximation of Eq. (8) implies that the 2p-2h states under consideration have quite similar 2p and 2h wave functions to the $N+2$ and $N-2$ isotopes, respectively. We illustrate this by first comparing the yrast spectra of ^{30}Ne (Table VI) and ^{32}Ne which has yrast $0^+,2^+,4^+,6^+,8^+,10^+$ levels at 0,1105,2211,3605,5213,6396 keV in rather remarkable agreement with the ^{30}Ne spectrum. The $0\hbar\omega$ yrast spectrum of ^{28}Ne is 0,1785,3300 keV for 0^+, 2^+, and 4^+ and hence will appear as nonyrast states in the $2\hbar\omega$ ^{30}Ne spectrum. Secondly, note that—as shown in Table VI—the $2_1^+\rightarrow 0_1^+$ and $4_1^+\rightarrow 2_1^+$ ^{32}Ne $B(E2)$ values (in e^2fm^4) are only $\sim 9\%$ smaller than those of ^{30}Ne.

The calculated wave functions of the $2\hbar\omega(2fp)$ lowest excited states in the $N=20$ isotones are as well deformed or more deformed than those of the known ground-state bands in this mass region. One can compare the calculated $E_x(2^+;2\hbar\omega)=1055$ keV for ^{30}Ne with those of the known ground bands. The lowest in the *sd* shell is $E_x=1274$ keV for ^{22}Ne, and lower energies are not found until $A>44$. One can also compare the β_2 deformation parameters as determined from the approximate relation

$$\beta_2=\frac{[B(E2;0^+\rightarrow 2^+)]^{1/2}}{(5/4\pi)Zr_{ch}^2}\ , \tag{11}$$

where the $B(E2)$ is in units of e^2fm^4 and r_{ch} is the rms charge radius in units of fm. With our calculated r_{ch} of 3.03 fm and $B(E2)=261$ e^2fm^4 for ^{30}Ne one obtains $\beta_2=0.44$. The largest value known for an *sd*-shell ground-state band is $\beta_2=0.50$ for ^{20}Ne [from experimental values of $r_{ch}=3.02$ fm (Ref. 52) and $B(E2)=327$ e^2fm^4 (Ref. 54)]. In the case of the known $4\hbar\omega$ excited-state band in ^{16}O, the relevant experimental quantities are $r_{ch}=2.71$ fm, $B(E2)=323\pm 36$ e^2fm^4, and $E_x(2^+;4\hbar\omega)=868$ keV (Refs. 52 and 54), which lead to $\beta_2=0.77$ and make this band appear "superdeformed" relative to the known ground-state band in ^{20}Ne and our proposed $2\hbar\omega$ band in ^{30}Ne (and ground-state band in ^{32}Ne).

We note here a difference in the weak-coupling analogy between ^{20}Ne vs ^{16}O($4\hbar\omega$) and ^{32}Ne vs ^{30}Ne($2\hbar\omega$). The weak-coupling model has been used to relate the excitation of the $4\hbar\omega$ state in ^{16}O to the binding energies of the $0\hbar\omega$ ^{16}O, ^{12}C, and ^{20}Ne states.[55] However, the fact that the $B(E2)$ is significantly larger in ^{16}O than in ^{20}Ne suggests considerable mixing of the $4\hbar\omega$ states within the weak-coupling basis. In contrast, our full calculation of the $2\hbar\omega$ states in ^{30}Ne compared to the states in ^{32}Ne suggests much less mixing and hence a better application of the weak-coupling model in our case. It would be interesting, but extremely difficult, to obtain experimental information in this $N=20$ mass region which would test these weak-coupling aspects of our results.

There is in fact no experimental information on $B(E2)$ values in the "island of inversion." There is one bit of information on the energy spectra which bears on collectivity; namely, the first-excited state of ^{32}Mg—presumably with $J^\pi=2^+$ and predominantly $2\hbar\omega$—was observed[4] at 885 keV. The $T(d_{3/2}f_{7/2}p_{3/2})$ prediction for the ^{32}Mg 2_1^+ energy of 1010 keV is not far from this value.

TABLE VII. Calculated quadrupole moments for the $2\hbar\omega$ 2_1^+ (even A) and $\frac{5}{2}_1^+$ (odd A) levels for the $A=28$–32 $N=20$ isotones. The $Q(E2)$ are in e fm^2 and are calculated with $\delta e_p=\delta e_n=0.35e$ in truncation (a) $T(1)$ and (b) $T(d_{3/2}f_{7/2}p_{3/2})$.

		$Q(E2)$	
A	Z	(a)	(b)
28	8	−2.80	+1.70
29	9	−11.95	−10.92
30	10	−10.78	−2.61
31	11		−1.74
32	12		−8.22

10. *Calculations of mixed (0+2)$\hbar\omega$ excitations*

In order to illustrate the "$n\hbar\omega$ truncation catastrophe" discussed in the Introduction, calculations were carried out in mixed $(0+2)\hbar\omega$ model spaces for the 0^+ states of ^{30}Ne. Three calculations were performed and are summarized in Table VIII. The results are as expected. Recall that the unperturbed $2\hbar\omega$ ground state lies 788 keV below the unperturbed $0\hbar\omega$ ground state (Fig. 4). Nevertheless, in the full $(0+2)\hbar\omega$ calculation the $0\hbar\omega$ amplitude dominates the ground state because the interaction with the high-lying $2\hbar\omega$ states of the same symmetry as the $0\hbar\omega$ ground state depresses the latter well below the unperturbed $2\hbar\omega$ state, i.e., this calculation lowers the ground state $\simeq 5$ MeV below the binding of the unperturbed $0\hbar\omega$ calculation (Table IV). Thus when the *fp-sd* energy gap is lowered by 2 MeV for the second calculation, the unperturbed $2\hbar\omega$ state (lowered by 4 MeV) is very close to the energy of the ground state which results from the interaction of the $0\hbar\omega$ ground state with high-

TABLE VIII. Results of mixed $(0+2)\hbar\omega$ calculations for the 0^+ states of ^{30}Ne. The full $0\hbar\omega$ model space is used for all three cases. The Full(-2) model space uses the full WBMB model space but with the energy gap between the *fp* and *sd* shells lowered by 2 MeV. The $T(d_{3/2}f_{7/2}p_{3/2})^*$ model space is that of $T(d_{3/2}f_{7/2}p_{3/2})$ with the *fp-sd* energy gap lowered by 1434 keV so that the unperturbed $2\hbar\omega$ E_{Bint} has the same value as for the full model space (see Table IV).

Model space	E_{Bint} (keV)	$E_x(0_2^+)$ (keV)	Percent $2\hbar\omega$ in 0_1^+
Full	94 943	4395	18.1
Full(-2)	06 064	1947	49.2
$T(d_{3/2}f_{7/2}p_{3/2})^*$	92 182	1781	25.2

lying $2\hbar\omega$ states, and the $0\hbar\omega$ and $2\hbar\omega$ ground states mix strongly. Reflection on these two calculations leads to the conclusion that the wave function of the $2\hbar\omega$ component in the mixed $(0+2)\hbar\omega$ ground state will be a strong function of the assumed *fp-sd* energy gap. The last model space calculation was made to illustrate that truncation lessens the "$n\hbar\omega$ truncation catastrophe," but does not remove it completely. That is, if there were no significant interaction of the $0\hbar\omega$ ground state with high-lying $2\hbar\omega$ states—or if a closely equal effect for the $2\hbar\omega$ ground state and high-lying $4\hbar\omega$ states were present—the ground state would be predominantly $2\hbar\omega$. This brings us to our final point of this exercise. There is no reason to suppose that the $(2+4)\hbar\omega$ effect would be equal to the $(0+2)\hbar\omega$ effect in a consistent calculation, i.e., one carried out to enough *n*p-*n*h terms (whatever that may be). Thus, even though the unmixed $2\hbar\omega$ calculation places the ground state below the unmixed $0\hbar\omega$ calculation, we do not know which amplitude would dominate the ground state in a consistent calculation.

V. DISCUSSION

A. Why is there an "island of inversion"?

We now discuss the mechanisms for lowering the $n\hbar\omega$ excitations which result in the island of inversion. The first thing to examine is the single-particle energy gap between the *sd* and *fp* shell. The neutron single-particle energies calculated with our interaction are given in Table IX, while in Fig. 6 we show these neutron single-particle energies relative to that of the $d_{3/2}$ orbit. For ^{28}O ($Z=8$) and ^{40}Ca ($Z=20$) the results are exact and given by $E(N=20;0\hbar\omega)-E(N=21;0\hbar\omega)$ for the *fp* particle states and by $E(N=20;0\hbar\omega)-E(N=19;0\hbar\omega)$ for the *sd* hole state. For ^{34}Si ($Z=14$) and ^{36}S ($Z=16$) the results are approximate and obtained under the assumption that the protons have a subshell closure of $(d_{5/2})^6$ and $(d_{5/2})^6(s_{1/2})^2$, respectively. Our full calculations for ^{34}Si and ^{36}S include all possible *sd*-shell proton configurations.

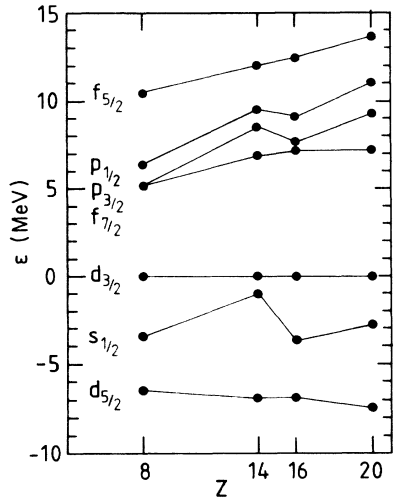

FIG. 6. Effective neutron single-particle energies relative to those of the $d_{3/2}$ orbit. From Table IX.

The gap between *sd* and *fp* shells shows a moderate decrease from $E_{gap}=7230$ keV in ^{40}Ca to 5115 keV in ^{28}O. This is in contrast to the results of Storm *et al.*,[8] which predict that the gap actually becomes negative for ^{28}O. Storm *et al.* do not present any experimental evidence to support their result. In contrast we see from Table II that our $0\hbar\omega$ mass predictions (and hence our single-particle energies) are in good agreement with experimental $N=19$, 20, and 21 binding energies from $Z=13$ to $Z=20$. Thus we have some confidence in the correctness of our extrapolation from $Z=12$ to $Z=8$. We conclude that the decrease in the *sd-fp* gap contributes but is not

TABLE IX. Effective single-particle energies. For ^{34}Si and ^{36}S, the proton $0d_{5/2}$ and $0d_{5/2}1s_{1/2}$ orbits, respectively, were constrained to be full. The Coulomb energy is not included and so for ^{16}O and ^{40}Ca the neutron (*n*) and proton (*p*) results are identical.

	^{16}O	^{28}O		^{34}Si		^{36}S	^{40}Ca
Orbit	*p*/*n*	*p*	*n*	*p*	*n*	*n*	*p*/*n*
$0d_{5/2}$	−3948	−22 959	−7414	−23 791	−16 080	−17 907	−23 014
$1s_{1/2}$	−3164	−20 100	−4391	−17 675	−10 175	−14 719	−18 326
$0d_{3/2}$	+1647	−16 205	−967	−15 757	−9212	−11 080	−15 596
$0f_{7/2}$	+5645	−8289	+4148		−2285	−3908	−8366
$1p_{3/2}$	+5172	−6476	+4223		−671	−3432	−6266
$1p_{1/2}$	+5160	−5681	+5400		+330	−1951	−4466
$0f_{5/2}$	+10 161	−2444	+9519		+2898	+1450	−1867
gap[a]	+9108	+14 670	+5115		+6927	+7172	+7230

[a]Gap is the energy difference between the highest occupied (or, for ^{16,28}O, the lowest available) positive-parity state and the lowest negative-parity state for the indicated particle.

the primary cause of the inversion.

For proton excitations we note that the gap between the $d_{5/2}$ and $f_{7/2}$ orbits is very large for ^{28}O (14.7 MeV), and *sd-fp* excitations for protons can be ignored, as we discussed in connection with the results of Table IV. Of course, the *sd-fp* gap is the same for protons and neutrons in ^{40}Ca and both excitations must be considered. However, as we also discussed in Sec. IV B 3, the low-lying $2\hbar\omega$ states in ^{38}Ar are already dominated by the excitation of neutrons.

The excitation energy of the $1\hbar\omega(1fp)$ neutron 1p-1h state in the $N=20$ isotones (see Fig. 5) is close to the gap energy $E_{\rm gap}$ for ^{28}O and not too different for ^{34}Si and ^{35}P. As Z increases, the lowering of the $1\hbar\omega(1fp)$ excitation to 2404 keV in ^{31}Na and its increase back up to 4747 keV in ^{34}Si is an aspect of the correlation energy (but on a smaller scale) which will now be discussed in some detail for the $2\hbar\omega$ excitations in $N=20$ and the $1\hbar\omega$ excitations in $N=19$ and 21.

First we consider the $2\hbar\omega$ excitations for $N=20$. It is noted from Fig. 4 that the excitation energy of the $2\hbar\omega$ neutron excitations is always much lower than twice the single-particle energy gap ($2\cdot E_{\rm gap}=2\cdot 5115$ keV in the case of ^{28}O). There are two factors which contribute to this lowering: (a) an increase in the neutron-neutron interaction energy E_{nn} and (b) the increase in the proton-neutron interaction energy E_{pn}. Since the monopole interaction is taken into account by the changes in the single-particle energies, E_{nn} is primarily due to the residual "pairing" interaction, and E_{pn} is primarily due to the residual $Q\cdot Q$ interaction.

E_{nn} can be estimated from the calculated excitation energy of the 2p-2h state in ^{28}O; $E_{nn}=E_x-2\cdot E_{\rm gap}=3038-2\cdot 5115$ keV $=-7192$ keV (with the weak-coupling estimate for E_x). Since E_{nn} only depends on the neutron configurations, we expect it to be approximately independent of Z. Thus the proton-neutron contribution E_{pn} as a function of Z can be estimated from $E_{pn}(Z)=E_x(Z)-2\cdot E_{\rm gap}-E_{nn}$ with $E_{\rm gap}=5115$ keV and $E_{nn}=-7192$ keV. For $Z=9$, 10, 11, 12, 13, and 14 we thus obtain $E_{pn}=-1752$, -3736, -3540, -3954, -2184, and -1222 keV, respectively. These turn out to be qualitatively similar to the "correlation" energy discussed by Poves and Retamosa[7] (see Fig. 2 of Ref. 7). However, a quantitative comparison cannot be made since the correlation energy is not well defined by Poves and Retamosa.

From the above analysis we can now see that there are three important mechanisms which combine to give the inversion of $2\hbar\omega$ relative to $0\hbar\omega$: the (small) reduction in the single-particle gap, the increase in the pairing energy E_{nn}, and the increase in the proton-neutron interaction energy E_{pn}. The only one which should have a strong Z dependence is E_{pn}.

When both protons and neutrons fill the beginning of a major shell there are strong α-type correlations which lead to well defined prolate deformations.[56] This is the case for ^{20}Ne and ^{24}Mg in the *sd* shell. When one or both types of particle are filling to the middle or end of a major shell there is a competition between prolate and oblate deformations as in the case of ^{28}Si, ^{32}S, and ^{36}Ar in the *sd* shell. In all $N=Z$ cases for $Z=10$–18 there are low-lying collective 2^+ states. The type and amount of collectiveness is sensitive to the degeneracy of the single-particle orbits in the major shell. The prolate deformation of ^{20}Ne and ^{24}Mg is reinforced by the nearness of the $d_{5/2}$ and $s_{1/2}$ orbits in the lower part of the *sd* shell.

For the $2\hbar\omega$ configurations in $N=20$, we note that the two-neutron configuration will always tend toward collectivity because the $f_{7/2}$ and $p_{3/2}$ neutrons orbits are close for all Z values (see Table IX). However, the situation for the two-proton configuration is quite different. At $N=20$ and $Z=8$ the $d_{5/2}$ orbits and $s_{1/2}$ proton orbits are close (see Table IX) and this reinforces the collectivity of the $(\nu fp)^2(\pi sd)^2$ configuration near ^{28}O. Hence E_{pn} is large for ^{30}Ne. However, as noted from Table IX, the gap between the $d_{5/2}$ and $s_{1/2}$ states increases to about 6 MeV for ^{34}Si. In this case the $d_{5/2}$ protons tend to form a closed shell, and the energy of the $0\hbar\omega$ 2^+ state in ^{34}Si is very high (4.9 MeV). Thus in the weak-coupling model the contribution to E_{pn} is greatly reduced, and would be zero in the limit of a $(d_{5/2})^6$ proton closed-shell configuration (since only the monopole term can contribute in this case). This is the reason for the strong Z dependence in E_{pn} and for the end of the island of inversion at ^{34}Si. As a consequence of the large $d_{5/2}-s_{1/2}$ proton splitting in ^{34}Si, the $d_{5/2}$ proton truncation assumed by Poves and Retamosa[7] may be partly useful for nuclei just below ^{34}Si (with some effective interaction changes), but closer to ^{28}O the explicit contribution from the proton $s_{1/2}$ orbit must be taken into account, and for the Gamow-Teller decay properties the $d_{3/2}$ orbit will always be important.

The E_{nn} contribution to the $1\hbar\omega$ excitation energy in the $N=19$ nuclei can be estimated from ^{27}O as $E_{nn}=E_x-E_{\rm gap}=2110-5115$ keV $=-2077$ keV. E_{pn} as a function of Z is then about -1448, -1899, -1804, -2102, -1151, and -1175 keV for ^{28}F, ^{29}Ne, ^{30}Na, ^{31}Mg, ^{32}Al, and ^{33}Si, respectively. The results for the $1\hbar\omega$ states of the $N=21$ nuclei are $E_{nn}=-4187$ keV and $E_{pn}(Z)=-304$, -1837, -1736, -1862, -1033, and -47 keV for ^{30}F, ^{31}Ne, ^{32}Na, ^{33}Mg, ^{34}Al, and ^{35}Si, respectively. The lowering of these states is due to the ^{3}He(^{3}H)-type correlation energy, and the relative magnitudes of these $E_{pn}(1\hbar\omega)$ relative to the $E_{pn}(2\hbar\omega)$ due to the α-type correlations discussed at the beginning of this section are reasonable. The inversion of the $2\hbar\omega$ excitations relative to $0\hbar\omega$ appears when the $0\hbar\omega$ ground state is itself not very collective. The reason why there is not an inversion of the $3\hbar\omega$ configuration relative to $1\hbar\omega$ in $N=19$ and 21 is probably because the $1\hbar\omega$ ground states are themselves already fairly collective.

It is well known that $n\hbar\omega$ spectra often lie very low in excitation energy for the reasons discussed above. The low-lying $4\hbar\omega$ 4p-4h state in ^{16}O and its explanation in terms of a weak-coupling model[55] is perhaps the most famous example. In fact, if the *p-sd* single-particle gap were only about 1 MeV smaller than what it actually is, this 4p-4h state would probably be the ground state of ^{16}O and the island of inversion near ^{31}Na would not be so

unique. The same can be said of ^{40}Ca. But by the time we reach $A=80$ the nominal shell closure of the fp shell is lost by the lowering of the $g_{9/2}$ orbit, and beyond this point it is well known that magic numbers are no longer those of the major harmonic-oscillator shell. The mechanisms behind our island of inversion are also responsible for the low-lying excited 0^+ states known in the Sn and Pb isotopes.[57] This suggests obvious applications of the weak-coupling approximation to these heavy nuclei.

B. Comparison to Poves and Retamosa

Considering the differences in model space and in approach, our results are in quite good agreement with those of Poves and Retamosa.[7] There are some points of difference. Their model space was $\pi d_{5/2}^{Z-8}\nu d_{3/2}^{N-18}(f_{7/2},p_{3/2})^2$ and the effects of this truncation can be seen if one looks at the $Q(E2)$ they found for ^{30}Ne (see the discussion in Sec. IV B 7). The major difference is in interpretation. It is difficult to reconcile their very low energy for the $2\hbar\omega$ 2^+ state (about 300 keV) with their moderate $B(E2)$ values—their $B(E2)$ values are only about half as large as ours (taking into account the difference between our effective charge of 0.35 and their effective charge of 0.5). Their very low 2^+ energy would suggest a "superdeformation" whereas their $B(E2)$ values suggest a very moderate deformation (about half that of ^{20}Ne). On the other hand, as discussed in Sec. IV B 7, both our 2^+ energy and $B(E2)$ value suggest a deformation comparable to that of ^{20}Ne.

C. Comparison of $1\hbar\omega$ and $2\hbar\omega$ binding energies to experiment

By considering $2\hbar\omega$ and $(1+3)\hbar\omega$ excitations we have achieved an understanding of the "island of inversion." What sort of quantitative agreement do we find between our predicted binding energies and experiment in the "island" region. A glance at Table II or Fig. 2 reveals that the USD does rather badly for the $0\hbar\omega$ binding energies of the $N=18$ isotones with $Z=9-13$. It overbinds them consistently. The reason for this is not known but is a subject for later study. If it is an N dependent effect of extrapolating away from stability then it could explain why the same trend is found for the WBMB predictions for $N=21-22$ (Sec. III). It also could mean that the overbinding in the "island" is worse than is apparent from the comparison shown in Table II. Keeping this in mind, we look at the $N=19-22$ Na and Mg isotopes. For $N=19$ our results are that the ground states could be either $0\hbar\omega$ or $1\hbar\omega$. In either case the $(n+2)\hbar\omega$ excitation lies close enough to explain the small discrepancy with experiment via the mutual repulsion of $n\hbar\omega$ and $(n+2)\hbar\omega$ states. Actually, the only serious disagreement with experiment for $N=19$ is that of ^{32}Al and for this case we have no explanation. For $N=20$ the situation is similar. Combining the results of Table II and Fig. 4, we find we underbind ^{31}Na and ^{32}Mg by 675 ± 492 and 375 ± 170 keV, respectively. Again, the small discrepancy is about what seems reasonable for the effects of mixing of $0\hbar\omega$ and $2\hbar\omega$ states. For $N=21$ and assumed $1\hbar\omega$ even-parity $Z=11$ and 12 ground states the discrepancies are 1185 ± 840 keV for ^{33}Mg and 3136 ± 740 keV for ^{32}Na. In both cases the unperturbed $0\hbar\omega$ ground state lies ~1 MeV higher. For ^{32}Na the discrepancy seems larger than can be explained by mixing. The case of odd-parity ground states is very similar and leads to the same discrepancies. Finally, for $N=22$ the disagreement for ^{33}Na is again very large, 3648 ± 1140 keV. The mass of ^{34}Mg is not known. It would seem that either there is some further experimental error in the very difficult measurements of these neutron-rich Na masses or we are missing an important ingredient in our calculation. One possibility for the latter is that $4\hbar\omega$ excitations are too important to neglect. We have shown (see Fig. 5) that $1\hbar\omega$ and $3\hbar\omega$ excitations lie close together in the "island." It seems remotely possible that a mixed $(0+2+4)\hbar\omega$ calculation could explain the observed binding. For $N=21$ and 22, a $4\hbar\omega$ calculation for Na is beyond our capabilities. For $N=20$, our weak-coupling prediction is that the unperturbed $4\hbar\omega$ state lies 3114 and 2509 keV above the unperturbed $2\hbar\omega$ state in ^{32}Na and ^{32}Mg, respectively. This does not seem close enough to give the necessary effect.

VI. SUMMARY

In this paper we have dealt in two subjects, (i) the development and predictive powers of a shell-model interaction, WBMB, operating in the model space of the $sdpf$ orbits, and (ii) the application of this interaction towards an understanding of the "island of inversion" centered at ^{32}Na. Let us summarize these two subjects in turn.

The WBMB interaction is tied tightly to the very successful USD interaction and its own success is certainly due to this connection. We have demonstrated in Sec. III its good predictive powers for the binding energies of $N>20$ nuclei. In previous publications its predictive powers for the binding energies of $1\hbar\omega(1fp)$ states in $N\leq20$ nuclei has been documented.[14,31,35,37,38] For all these configurations its predictive power for other observables is also good.[14,31,35,37,38,51] Besides its close ties to the USD interaction, another reason for its success is the inclusion of the full sd and fp major shells in its model space. Thus it is applicable over a large range of Z and N and the inclusion of all spin-orbit partners renders it suitable for the calculation of $M1$-like observables as well as the matrix elements occurring in first-forbidden beta decay.[14,51]

Now consider application of the WBMB to the "island of inversion." One price we must pay for our desire to stay as close as possible to a full $sdpf$ model space is large and time-consuming calculations. Poves and Retamosa,[7] using the $\pi d_{5/2}^{Z-8}\nu d_{3/2}^{N-18}(f_{7/2},p_{3/2})^2$ model space had, at maximum, $D(J)=800$. By contrast we have diagonalized up to $D(J)=11\,000$ and that, in fact, has been the restriction on the extent of our calculations.

We have given reasons (Secs. I and IV B 10) why we have not tried to calculate mixed $(0+2)\hbar\omega$ configurations

in a serious manner. Our interaction is not designed for it. It is conceivable that an effective $(0+2)\hbar\omega$ interaction for the full *sdpf* model space could be derived in which the effects of $>2\hbar\omega$ excitations were included by an effective adjustment of the interaction just as $>0\hbar\omega$ excitations are included in the standard interaction. There is much current interest and activity in this direction. However, it is too early to tell how well this approach will work.

We have found that the "island of inversion" is probably confined to the nine nuclei indicated in Fig. 1, although we were unable to clearly demonstrate that ^{34}Na and ^{35}Mg are not included. This conclusion was also reached by Poves and Retamosa[7] who also did not calculate the $N=23$ isotones. Although we are successful in finding an "island" and understanding its reasons (Sec. V A), there is one serious disagreement with experiment; namely, the underbinding of ^{32,33}Na.

Our understanding of the "island of inversion" is presently hampered by lack of experimental information. Remeasurement of the masses of ^{32,33}Na would be extremely valuable. So would a determination of the parties of the ^{30,32}Na and ^{31,33}Mg ground states for which we find very closely competing ground states. These measurements are presently possible; more difficult but just as valuable would be an extension of the known Ne masses past $N>20$.

ACKNOWLEDGMENTS

We thank D. J. Millener for valuable discussions and A. Poves for an informative communication. Research was supported by the U.S. Department of Energy under Contract No. DE-AC02-76CH00016 with Brookhaven National Laboratory and Contract No. W-7405-Eng-48 with the University of California (Lawrence Livermore National Laboratory) and in part by the National Science Foundation under Grant No. PHY-87-14432 with Michigan State University. One of us (E.K.W.) is grateful for an Alexander von Humboldt-Stiftung which supported that part of the research carried out at Heidelberg University and the Max Planck Institute.

[1]C. Thibault, R. Klapisch, C. Rigaud, A. M. Poskanzer, R. Prieels, L. Lessard, and W. Reisdorf, Phys. Rev. C **12**, 644 (1975).

[2]X. Campi, H. Flocard, A. K. Kerman, and S. Koonin, Nucl. Phys. **A251**, 193 (1975).

[3]C. Détraz, M. Langevin, M. C. Goffri-Kouassi, D. Guillemaud, M. Epherre, G. Audi, C. Thibault, and F. Touchard, Nucl. Phys. **A394**, 378 (1983).

[4]C. Détraz, D. Guillemaud, G. Huber, R. Klapisch, M. Langevin, F. Naulin, C. Thibault, L. C. Carraz, and F. Touchard, Phys. Rev. C **19**, 164 (1979).

[5]B. H. Wildenthal and W. Chung, Phys. Rev. C **22**, 2260 (1980).

[6]A. Watt, R. P. Singhal, M. H. Storm, and R. R. Whitehead, J. Phys. G **7**, L145 (1981).

[7]A. Poves and J. Retamosa, Phys. Lett. B **184**, 311 (1987).

[8]M. H. Storm, A. Watt, and R. R. Whitehead, J. Phys. G **9**, L165 (1983).

[9]A. De-Shalit and M. Goldhaber, Phys. Rev. **92**, 1211 (1953).

[10]P. Federman and S. Pittel, Phys. Rev. C **20**, 820 (1979).

[11]P. J. Ellis and L. Zamick, Ann. Phys. (N.Y.) **55**, 61 (1969).

[12]D. J. Millener, private communication.

[13]E. K. Warburton, D. E. Alburger, J. A. Becker, B. A. Brown, and S. Raman, Phys. Rev. C **34**, 1031 (1986).

[14]E. K. Warburton, J. A. Becker, D. J. Millener, and B. A. Brown, *The WBMB Shell-Model Interaction and the Structure of $^{16}O(2s,1d)^{A-16-n}(1f,2p)^n$ Levels in $A=31-44$ Nuclei with Particular Emphasis on Binding Energies and Energy Spectra*, BNL Report 40890, 1987.

[15]B. H. Wildenthal, Prog. Part. Nucl. Phys. **11**, 5 (1984).

[16]J. P. McGrory, Phys. Rev. C **8**, 693 (1973).

[17]D. J. Millener and D. Kurath, Nucl. Phys. **A255**, 315 (1975).

[18]B. A. Brown and B. H. Wildenthal, Annu. Rev. Nucl. Sci. **38**, 29 (1988).

[19]T. T. S. Kuo and G. E. Brown, Nucl. Phys. **A85**, 40 (1967).

[20]S. Cohen and D. Kurath, Nucl. Phys. **73**, 1 (1965).

[21]T. T. S. Kuo, Nucl. Phys. **A103**, 71 (1967).

[22]The sensitivity of the "1p-1h" spectra of ^{16}O and ^{40}Ca to the parameters of the Millener-Kurath potential was examined by varying one at a time and examining the change in the spectra. From this study it was found that some improvement could be had by giving some terms of the potential two or three range components and possibly including some density dependence. For ^{40}Ca, a general increase in the strength of the interaction by $\sim 15\%$ would also lead to improvement.

[23]W. Chung, Ph.D. thesis, Michigan State University, 1976.

[24]A comprehensive report of results of the USD interaction (Ref. 15) had not yet been published. However, a summary of binding energies for $A=17-39$ nuclei has been privately circulated. A description of the method used to calculate the Coulomb contribution to the experimental binding energy is given in Ref. 23.

[25]B. A. Brown, A. Etchegoyen, W. D. M. Rae, and N. S. Godwin, OXBASH, 1984 (unpublished).

[26]D. H. Gloeckner and R. D. Lawson, Phys. Lett. **53B**, 313 (1974).

[27]P. M. Endt and C. van der Leun, Nucl. Phys. **A310**, 1 (1978).

[28]G. Huber, F. Touchard, S. Buttgenbach, C. Thibault, R. Klapisch, H. T. Duong, S. Liberman, J. Pinard, J. L. Vialle, P. Juncar, and P. Jacquinot, Phys. Rev. C **18**, 2342 (1978).

[29]D. Guillemaud, C. Détraz, M. Langevin, F. Naulin, M. de Saint-Simon, C. Thibault, F. Touchard, and M. Epherre, Nucl. Phys. **A426**, 37 (1984).

[30]D. R. Goosman and D. E. Alburger, Phys. Rev. C **7**, 2409 (1973).

[31]E. K. Warburton and J. A. Becker, Phys. Rev. C **37**, 754 (1988).

[32]P. Baumann, A. Huck, G. Klotz, A. Knipper, G. Walter, G. Marguier, H. L. Ravn, C. Richard-Serre, A. Poves, and J. Retamosa, Phys. Lett. B **228**, 458 (1989).

[33]D. R. Goosman, C. N. Davids, and D. E. Alburger, Phys. Rev. C **8**, 1331 (1973).

[34]L. K. Fifield, C. L. Woods, W. N. Catford, R. A. Bark, P. V. Drumm, and K. T. Keoghan, Nucl. Phys. **A453**, 497 (1986).

[35]E. K. Warburton and J. A. Becker, Phys. Rev. C **35**, 1851 (1987).

[36]C. E. Thorn, J. W. Olness, E. K. Warburton, and S. Raman,

Phys. Rev. C **30**, 1442 (1984).
[37]E. K. Warburton and J. A. Becker, Phys. Rev. C **39**, 1535 (1989).
[38]E. K. Warburton and J. A. Becker, Phys. Rev. C **40**, 2823 (1989).
[39]A. H. Wapstra, G. Audi, and R. Hoekstra, At. Data Nucl. Data Tables **39**, 281 (1988).
[40]J. M. Wouters, R. H. Kraus, Jr., D. J. Vieira, G. W. Butler, and K. E. G. Lobner, Z. Phys. A **331**, 229 (1988).
[41]D. J. Vieira, J. M. Wouters, K. Vaziri, R. H. Kraus, H. Wollnik, G. W. Butler, F. K. Wohn, and A. H. Wapstra, Phys. Rev. Lett. **57**, 3253 (1986).
[42]A. Gillibert, W. Mittag, L. Bianchi, A. Cunsolo, B. Fernandez, A. Foti, J. Gastebois, C. Grégoire, Y. Schutz, and C. Stephan, Phys. Lett. B **192**, 39 (1987).
[43]L. K. Fifield, R. Chapman, J. L. Durell, J. N. Mo, R. J. Smith, P. J. Woods, B. R. Fulton, R. A. Cunningham, and P. V. Drumm, Nucl. Phys. **A484**, 117 (1988).
[44]P. V. Drumm, L. K. Fifield, R. A. Bark, M. A. C. Hotchkis, and C. L. Woods, Nucl. Phys. **A469**, 530 (1989).
[45]In this study a definite difference in the average *fp-sd* energy gap was found between the neutron-rich nuclei—for which only the $T=1$ hole-particle interaction is operative—and the $N \leq 20$ nuclei for which both $T=0$ and 1 interactions come into play. For the $N > 20$ nuclei of Table II, the "best" *fp-sd* energy gap is 113 keV larger than the value found from all nuclei considered.
[46]P. Möller, W. D. Myers, W. J. Swiatecki, and J. Treiner, At. Data Nucl. Data Tables **39**, 225 (1988).
[47]E. K. Warburton and D. J. Millener, Phys. Rev. C **39**, 1120 (1989).
[48]R. D. Lawson, *Theory of the Nuclear Shell Model* (Oxford University, New York, 1980), and references therein.
[49]P. Baumann, Ph. Dessagne, A. Huck, G. Klotz, A. Knipper, C. Miehé, M. Ramdane, G. Walter, G. Marguier, H. Gabelmann, C. Richard-Serre, K. Schlösser, and A. Poves, Phys. Rev. C **39**, 626 (1989).
[50]P. Baumann, Ph Dessage, A. Huck, G. Klotz, A. Knipper, G. Marguier, C. Miehé, M. Ramdane, C. Richard-Serre, G. Walter, and A. Poves (unpublished).
[51]E. K. Warburton, J. A. Becker, B. A. Brown, and D. J. Millener, Ann. Phys. (N.Y.) **187**, 471 (1988).
[52]B. A. Brown, C. R. Bronk, and P. E. Hodgson, J. Phys. G **10**, 1683 (1984).
[53]This observation and others given below on the effects of truncation can be better understood after consideration of the effective single-particle energies which is given in Sec. V A.
[54]F. Ajzenberg-Selove, Nucl. Phys. **A460**, 1 (1986); **A475**, 1 (1987).
[55]L. Zamick, Phys. Lett. **19**, 580 (1965).
[56]A. Bohr and B. R. Mottleson, *Nuclear Structure* (Benjamin, Reading, 1975), Vol. 2, p. 99.
[57]K. Heyde, J. Jolie, J. Moreau, J. Ryckebusch, M. Waroquier, P. Van Duppen, M. Huyse, and J. L. Wood, Nucl. Phys. **A466**, 189 (1987).